Journal of Proteomics 143 (2016) 173–187

Contents lists available at ScienceDirect

Journal of Proteomics

journal homepage: www.elsevier.com/locate/jprot

Microbial symbionts affect *Pisum sativum* proteome and metabolome under *Didymella pinodes* infection

G. Desalegn [a,1], R. Turetschek [b,1], H.-P. Kaul [a], S. Wienkoop [b,*]

[a] University of Natural Resources and Life Sciences, Department of Crop Sciences, Austria
[b] University of Vienna, Department of Ecogenomics and Systems Biology, Austria

ARTICLE INFO

Article history:
Received 18 December 2015
Received in revised form 18 February 2016
Accepted 15 March 2016
Available online 22 March 2016

Keywords:
Biotic stress
Didymella pinodes
Field pea
Mycorrhiza
Rhizobia
Inoculation
Photosynthesis
Biomass
Proteome
Metabolome

ABSTRACT

The long cultivation of field pea led to an enormous diversity which, however, seems to hold just little resistance against the ascochyta blight disease complex. The potential of below ground microbial symbiosis to prime the immune system of *Pisum* for an upcoming pathogen attack has hitherto received little attention. This study investigates the effect of beneficial microbes on the leaf proteome and metabolome as well as phenotype characteristics of plants in various symbiont interactions (mycorrhiza, rhizobia, co-inoculation, non-symbiotic) after infestation by *Didymella pinodes*. In healthy plants, mycorrhiza and rhizobia induced changes in RNA metabolism and protein synthesis. Furthermore, metal handling and ROS dampening was affected in all mycorrhiza treatments. The co-inoculation caused the synthesis of stress related proteins with concomitant adjustment of proteins involved in lipid biosynthesis. The plant's disease infection response included hormonal adjustment, ROS scavenging as well as synthesis of proteins related to secondary metabolism. The regulation of the TCA, amino acid and secondary metabolism including the pisatin pathway, was most pronounced in rhizobia associated plants which had the lowest infection rate and the slowest disease progression.

Biological significance: A most comprehensive study of the *Pisum sativum* proteome and metabolome infection response to *Didymella pinodes* is provided. Several distinct patterns of microbial symbioses on the plant metabolism are presented for the first time. Upon *D. pinodes* infection, rhizobial symbiosis revealed induced systemic resistance e.g. by an enhanced level of proteins involved in pisatin biosynthesis.

1. Introduction

Legume crops such as field peas (*Pisum sativum* L.) are important components of the human and animal diet due to their content of protein, starch and other nutrients as well as their health benefit potentials. However, various aspects of field pea growth, development, productivity and expansion are threatened by abiotic and multiple biotic (pathogens or insects) stresses, of which Ascochyta blight is the most important necrotrophic foliar disease in most pea growing regions [1,2]. Particularly, *Didymella pinodes* (synonym: *Mycosphaerella pinodes*) which attacks seedlings and all the above ground parts of pea plants [3] is the most damaging one [4]. The two major damaging effects of this disease on crop growth distinguished by Shtienberg [5] were decreases in leaf area and photosynthetic efficiency of the remaining green leaf area. It has been reported that biotic stress globally downregulates photosynthetic genes [6]. *D. pinodes* alters carbohydrate metabolism, protein remobilization and free amino acid translocation from diseased leaves, what is likely to reduce photosynthesis [7] and causes significant yield losses. As reviewed by McDonald and Peck [8], between 30% and 75% losses have been measured in Australia, France and Canada. Although extensive breeding studies have been carried out, pea cultivars with durable resistance to *D. pinodes* are not yet available [1,9]. To reduce disease severity, minimise yield losses and improve the crop's contribution to food security, the suggested control measures are fungicide use and agronomic practices (burial or burning of infected crop residues, use of a suitable crop rotation and shifting of sowing dates). However, these control measures imply environmental threats (e.g. toxicity) or are often not suitable to many farm situations (e.g. sowing date). Therefore, alternative sustainable practices for pea production need to be developed and expanded.

Previously, the positive contribution of beneficial microbes for improving plant health, growth, development and productivity has been extensively reported, especially arbuscular mycorrhiza fungi (AMF) and rhizobia associations in the rhizosphere [9–11]. Plant growth-promoting rhizobacteria can induce systemic resistance in plants and minimise disease severity in both roots and leaves [12]. Likewise, phytohormones released from microorganisms activate plant immunity [13].

Recently, Kosova et al. and Perez-Alfocea et al. [14,15] reported that plant acclimation to stress is associated with profound changes in composition of the plant transcriptome, proteome, and metabolome.

* Corresponding author.
E-mail address: stefanie.wienkoop@univie.ac.at (S. Wienkoop).
[1] Authors contributed equally.

http://dx.doi.org/10.1016/j.jprot.2016.03.018

Presumably, such changes could be affected by belowground microbial symbionts (e.g. AMF and/or rhizobia). The research on crop plants progressively enters the field of proteomics [16], and methods were proposed to analyse the proteome of non-model organisms [17,18]. In recent years, the main goals of proteomics [19] and its advancement in techniques and protocols for high-throughput proteomics are extensively presented [20]. In the investigation of symbiotic and plant–pathogen interactions, proteomics especially proved to be a successful approach to understand molecular mechanisms [21,22]. Similarly, metabolomics has a promising role in agriculture to unravel responses of stressed plants [23] or to assign plant molecular modifications associated with symbionts [24]. Besides the biosynthesis of secondary metabolites, the regulation of primary metabolites is known to crucially contribute to the plants' defence response [25]. The integration of proteomic and metabolomic data was prioritized frequently [26,27] to obtain a systemic view of the plants' molecular adjustment.

In the past, most reports claimed for synergistic effects of co-inoculation of AMF and rhizobia on legume growth and development [28–33], because of enhanced N uptake or N_2-fixation [34,35]. However, other studies showed a negative effect of mycorrhiza on nodule development and legume plant growth [36–38]. In general, the productivity of a legume crop cultivar depends on the effectiveness and compatibility of the AMF [39] and the *Rhizobium* bacteria in the rhizosphere [29]. So far, information on the priming effects of AMF and rhizobia, particularly on the proteome and metabolome of field pea under biotic and abiotic stresses, is scarce.

Hence, in this study, we investigated:

1) Whether the bipartite- (peas–mycorrhiza or peas–rhizobia) or tripartite-interactions (peas–mycorrhiza–rhizobia) affect the pea leaf proteome and metabolome compared to non-symbiotic plants.
2) Whether these interactions interfere with the plants phenotypic and molecular response to *D. pinodes* infection.

Hence, with this study we aim to provide new insights into potential benefits of microbial symbionts to develop induced systemic resistance in pea plants against *D. pinodes*. This knowledge contributes to breeding strategies in order to improve field pea productivity, yield security and expansion in cropping systems globally.

2. Materials and methods

2.1. Materials and plant growth conditions

2.1.1. Experimental design and soil conditions

In an effort to investigate whether a single or dual inoculation of arbuscular mycorrhiza fungi (AMF) and rhizobia affect dry matter, photosynthetic components (e.g. green area), as well as the proteome and the metabolome of pea plants, a factorial experimental design with four treatments and two biotic conditions was carried out in a randomized complete block design. The four treatments were: AMF, *Glomus mosseae* (M), *Rhizobium leguminosarum* bv. *viceae* (R), dual microbial symbionts of AMF and *Rhizobium* (MR) and a control with dual synthetic NP mineral fertilizer but without symbionts (NS). Four or three biological replicates were sampled for phenotypic characterisation as well as for proteomic and metabolomic studies, respectively.

The soil used in this experiment was collected from the 0–20 cm horizon of arable fields in Tulln, Austria. Table S1 shows its chemical and physical characteristics. It was air-dried, sieved to pass a 2 mm sieve, mixed with expanded clay and silica sand (1:1:1 w/w/w), and sterilised at 121 °C for 20 min. Prior to planting, plastic pots (3 L) were disinfected with 12% sodium hypochlorite, cleaned with deionised water, filled with 2 kg growing substrate (described below) and moistened with 400 mL sterilised deionised water. To maintain the moisture content at optimum levels, pots were irrigated with sterilised deionised water every second day until a drop came out from their bottom. As can be seen from Table S1, the soil was low in both plant available nitrogen and phosphorus. In low N soils, a starter dose as little as 5–10 kg N ha^{-1} can stimulate seedling growth and early nodulation such that both N_2 fixation and eventual yield are enhanced [40]. The same is true for phosphorus and AM-symbiosis.

Therefore, each pot received starter N and P with synthetic fertilizers at the same rate of 20 mg kg^{-1} soil after planting. Furthermore, the non-symbiotic treatment received N and P forms as described by Hoffmann et al. [41] for beans (i.e., 80 mg N and 28 mg P kg^{-1} soil). Similar to this dual NP mineral fertilizer group, pots with single AM fungi or single *Rhizobium* bacteria treatment also received nitrogen or phosphorus, respectively. Additionally, a modified NP free nutrient solution prepared according to Broughton and Dilworth [42] ($CaCl_2$ 147 ppm, Fe-citrate 3.35 ppm, $MgSO_4 \cdot 7H_2O$ 61.6 ppm, K_2SO_4 43.5 ppm, $MnSO_4$ 0.17 ppm, H_3BO_3 0.123 ppm, $ZnSO_4$ 0.144 ppm, $CuSO_4$ 0.05 ppm, $CoSO_4$ 0.028 ppm, $NaMoO_2$ 0.024 ppm; pH 6.7) was applied at a rate of 10 mL pot^{-1} once a week.

2.1.2. Biological materials

Commercial inoculants (Vaminoc) containing a *Glomus* species and a *R. leguminosarum* bv. *viceae* were obtained from former Becker Underwood Ltd. UK. The inoculants were applied as prescribed by the company. The *P. sativum* seeds obtained from Rubiales Lab, Cordoba (Spain) was cultivar Messire, which is reported to be susceptible to *D. pinodes* [1,43,44]. From the bulk seeds, we selected uniform and healthy ones for surface sterilisation (70% ethanol for 30 s, 12% sodium hypochlorite for 5 min). Subsequently, the seeds were rinsed six times with sterilised deionised water, and pre-germinated in previously autoclaved (20 min at 121 °C) perlite. From three days old pre-germinated seeds, five healthy-looking plantlets pot^{-1} were chosen. To avoid potential cross-contamination of microbial inoculants between treatments, planting and covering of the germinated seeds were started with NS pots. Ten days after planting, seedlings were thinned down to three and four

Table 1
Plasma membrane proteins significantly responding to infection (Student's *t*-test, $p < 0.05$).

Accession	Description	Peptides	Max. peptide Score	i/h		
				p-Val (*p*-adjust)	Ratio	Significance
gi|118933	Disease resistance response protein Pi49 (PR10)	13	252.12	0.000 (0.007)	7.8	***
gi|1708427	2′-Hydroxyisoflavone reductase (NADPH: isoflavone oxidoreductase)	22	255.39	0.004 (0.062)	5.3	**
gi|257632899	Unnamed protein product [*Pisum sativum*]	16	179.65	0.000 (0.001)	6.7	***
frv2_47806	Plastocyanin-like domain protein (UniRef100_A0A072TWJ3 icov:100% qcovs: 73.98% e-val: 6e-78)	4	174.94	0.000 (0.007)	8.9	***
frv2_110760	12-Oxophytodienoate reductase-like protein(UniRef100_G7K3S2 icov: 96% qcovs: 91.11% e-val: 0)	9	165.89	0.002 (0.042)	3.9	**
frv2_111907	Archaeal/vacuolar-type H^+-ATPase subunit B (UniRef100_A0A072VSL4 icov: 98% qcovs: 99.18% e-val: 0)	17	206.74	0.013 (0.178)	3.5	*
frv2_53662	Protein disulfide-isomerase (UniRef100_B7FM01 icov: 98% qcovs: 84.41% e-val: 0)	17	202.4	0.018 (0.213)	2.3	*
frv2_75243	Translational elongation factor 1 subunit Bbeta (UniRef100_Q6SZ89 icov: 90% qcovs: 95.67% e-val: 3e-133)	5	187.78	0.003 (0.051)	2.1	**
frv2_83550	PfkB family carbohydrate kinase (UniRef100_G7IAA1 icov: 91% qcovs: 92.08% e-val: 0)	10	314.42	0.000 (0.007)	2.5	***
frv2_86187	Glucan endo-1,3-beta-d-glucosidase (UniRef100_Q9ZP12 icov: 98% qcovs: 87.01% e-val:0)	11	307.43	0.000 (0)	2.4	***
frv2_86875	Proteasome subunit beta type (UniRef100_B7FGZ8 icov: 85% qcovs: 96.98% e-val: 4e-164)	4	192.4	0.001 (0.015)	2.4	***

plants pot^{-1} for morphological characterisation and for proteomic/metabolomic studies, respectively. Pots were arranged on benches at 20 °C day and 12 °C night temperature. Relative humidity was at 60 ± 5% with 14 h photoperiod and a light intensity of 300 μmol m^{-2} s^{-1}. 1. Pots were rotated every ten days.

A pathogen inoculum of pea plants (i.e. *D. pinodes* isolate) was also obtained from the Rubiales Lab, Cordoba (Spain), and multiplied in Petri dishes containing PDA media (23 °C, 12 h photoperiod). Approximately thirty days after planting (at the 8th to 10th leaf stage), plants were inoculated by spraying a conidia suspension containing 5 × 10^6 conidia mL^{-1} and 120 μL of Tween-20 in 100 mL as a wetting agent. After inoculation, plants were covered with a polyethylene sheet. High humidity was ensured by adjustable and automatic humidifiers operating for 15 min every 2 h in the controlled greenhouse.

2.2. Assessment of phenotypic characteristics

2.2.1. Plant disease severity

After the initial 36 h the polyethylene cover was removed and plants were maintained in the controlled greenhouse throughout disease development and assessment and any other measurements. For assessment disease severity (DS), two scorings (i.e., on day three and nine after *D. pinodes* inoculation) were performed as described by Roger and Tivoli [45]. Visual estimation of the percentage of the plant surface covered by symptoms, such as on stipules and leaflets at first, fourth and eighth nodes and the plants' mean were taken using a 0–5 scale (0, no lesion; 1, a few scattered flecks; 2, numerous flecks; 3, 10–15% leaf area necrotic and appearance of flecks; 4, 50% of leaf area covered by lesions; 5, 75–100% of leaf area dehydrated or necrotic).

2.2.2. Microbial symbionts' effectiveness and plant growth components

At full flowering stage (BBCH 65) plants were cut at ground level, the shoot fresh weight was taken, subsequently all the dead leaves or not green ones and flowers were removed, and the green area was measured using a scanning planimeter (LI-COR 3100 area meter, Lincoln, NE, USA). Finally, for dry matter (DM) determination, all shoot parts were dried at 40 °C for five days.

Mycorrhizal root colonisation and *Rhizobium* root nodulation were assessed after rinsing off the remaining substrate on the roots with running tap water on a fine (1 mm) sieve bench in the root washing facility. For mycorrhizal colonisation assessment, roots were cleared and stained according to Vierheilig et al. [46] by boiling them in 10% KOH for 10 min and in a 5% ink (Schaeffer black ink) plus household vinegar (equal to 5% acetic acid) solution for 5 min. The percentage of root length colonised by AMF was estimated according to Newman [47]. For *Rhizobium* nodulation assessment, nodules were removed from the roots, to record their number as well as fresh weight and dried after five days at 40 °C.

2.3. Proteome and metabolome studies

2.3.1. Plant sampling and preparation

For proteomic and metabolomic studies, plants were sampled at 36 h (late morning hours) after infection in order to obtain the least circadian effect on the proteome/metabolome. It was reported that *D. pinodes* penetrates the leaf cuticle after 24 h and small lesions become visible [43,48] and infection is in general most effective in the evening. Three pots were sampled each representing one biological replicate. Leaves from 3 out of 4 plants per pot were pooled to eliminate effects of a varying infection success. The fourth plant was used for extraction of the plasma membrane (Section 2.3.3). After immediate quenching in liquid nitrogen, leaves were ground to a fine powder in liquid nitrogen and then samples were stored at −80 °C for further processing.

2.3.2. Integrative extraction of metabolites and proteins

About 25 mg fresh weight of the ground samples were used for extraction with 1 mL of freshly prepared and pre-cooled extraction buffer (MeOH:$CHCl_3$:H_2O, 2.5:1:0.5). Samples were kept on ice for 8 min with regular agitation before centrifugation (4 min, 14,000 *g*, 4 °C). The supernatant was transferred to a new tube containing 500 μL ultrapure water and shaken thoroughly. After centrifugation (4 min, 14,000 *g*, 4 °C) the upper phase, containing polar metabolites, was split into two aliquots and dried in a vacuum concentrator. The remaining plant material was kept for further extraction of proteins (Section 2.3.2.2).

2.3.2.1. Derivatisation and analysis with GC–MS. Vacuum dried metabolites were dissolved in 20 μL of a 40 mg mL^{-1} solution methoxyamine hydrochloride in pyridine through shaking at 30 °C for 90 min *N*-methyl-*N*-trimethylsilyltrifluoroacetamid (40 μL) spiked with 60 μL/mL of an even-numbered alkane mix (C10–C40) was added followed by incubation for 30 min at 37 °C under continuous shaking and centrifugation at 14,000 *g*. The supernatant was transferred into a glass vial for measurement. The sample (1 μL) was injected into a GC coupled triple quadrupole (Thermo Scientific TSQ Quantum GC™, Bremen, Germany). GC and MS adjustments were set as described by Staudinger et al. [49] with minor variations. To enable the quantification of sugars, the samples were measured in split less and split mode with a ratio of 10. Before and after a set of 10 randomly queued samples a set of 5 different concentrations of external standard mix was measured. Identification was based on the matching of MS-spectra and retention time index (calculated through the spiked alkane mix) against an in-house library (extended gmd database) in AMDIS [43]. Peak areas were integrated with the software LCquan (version 2.5, Thermo Xcalibur). Absolute metabolite quantities were calculated by normalization to the slope of the external standard and to the fresh weight. Metabolites not found in the external standard were normalized to the slope of a similar substance with nearby retention time (e.g. nicotinate was normalized to the slope of citric acid).

2.3.2.2. Integrative protein extraction. Proteins were extracted from the plant material pellet (2.4.1) using trizol (TRI Reagent®, Sigma-Aldrich) according to Carrillo et al. [43], with minor modifications. The plant material left over from metabolite extraction was sonicated in 800 μL trizol reagent. For phase separation of phenolic and water soluble compounds 160 μL of chloroform was added prior centrifugation (15 min, 12,000 *g*, 4 °C). The upper aqueous phase was discarded and 240 μL EtOH were added to facilitate pelleting of the insoluble leaf material by centrifugation (5 min, 7000 *g*, 4 °C). The supernatant was transferred and proteins were precipitated overnight with five times of the initial volume in −20 °C cold acetone containing 0.5% β-mercaptoethanol. The precipitate was pelleted (10 min, 4000 *g*, 4 °C), subsequently the supernatant removed and the protein pellet dissolved in 700 μL urea buffer (8 M urea, 50 mM HEPES, pH 7.8).

2.3.3. Plasma membrane preparation

The fresh leaves of one plant (2–4 g) were homogenized in breaking buffer (0.1 M HEPES, 1 mM EDTA, 0.33 M sucrose, 5 mM DTT, 1.5% PVPP, 1 mM PMSF, pH 7.5). The homogenate was centrifuged for 30 min at 30,000 *g* to pelletise the microsomal fraction, consisting of membranes derived from different vesicles. The supernatant (fraction with the cytosol) was precipitated and dissolved in urea buffer as described for the integrative protein extraction. Plasma membranes in the microsomal fraction were purified by use of an aqueous two phase partitioning optimized for *Pisum l*eaves according to Luthje et al. [50].

2.3.4. Protein digestion

Protein concentration was determined via Bradford assay [49] and a BSA standard calibration line. A volume corresponding to 100 μg (integrative extraction and cytosolic fraction) and 20 μg (plasma

membrane) proteins was transferred and LysC (1:100 vol/vol, 5 h, 30 °C, Roche, Mannheim, Germany) was added for initial digestion. Samples were diluted with trypsin buffer (10% ACN, 100 mM AmBic, 1 mM $CaCl_2$, 5 mM DTT) to a final concentration of 2 M urea and incubated over night at 37 °C with Poroszyme immobilized trypsin beads (1:10, vol/vol; Applied Biosystems, Darmstadt, Germany). The digest was applied on C18-SPEC 96-well plates (Varian, Darmstadt, Germany) and washed twice with 250 μL water. The sample flow-through and the first wash step were kept for second desalting step with graphite. Peptides were eluted from C18-spec-plates with 500 μL of 100% MeOH. Proteins from the flow through and the first wash step were desalted with 10 mg graphite in spin columns (MobiSpin Column F, MoBiTec) according to the manufacturer's instructions (Thermo scientific, Pierce® graphite spin columns). Eluates from graphite and C18 desalting were subsequently merged, split into two technical aliquots, and dried in a vacuum concentrator.

2.3.5. Nano ESI LC–MS/MS

Peptides were dissolved in 100 μL 2% ACN, 0.1% FA and 1 μg of each sample were applied randomly on a reverse phase C18 column. Integrative extracted peptides (3 biological and 2 technical replicates) were loaded on a 15 cm × 50 μm column (PepMap®RSLC, Thermo scientific, 2 μm particle size) and separated during a 90 min gradient with a flow rate of 300 nL min^{-1}. MS measurement was performed on an LTQ-Orbitrap Elite (Thermo Fisher Scientific, Bremen, Germany) with the following settings: Full scan range 350–1800 *m/z*, max. 20 MS2 scans (activation type CID), repeat count 1, repeat duration 30 s, exclusion list size 500, exclusion duration 60 s, charge state screening enabled with rejection of unassigned and +1 charge states, minimum signal threshold 10,000.

Cytosolic peptides (3 biological and 2 technical replicates) and plasma membrane peptides (3 biological replicates) were applied on a 15 cm × 100 μm column (Supelco Ascentis® Express Peptide ES-C18, 2.7 μm particle size) for separation during a 90 min gradient with a flow rate of 400 nL min^{-1}. MS measurement was performed on an LTQ-Orbitrap XL (Thermo Fisher Scientific, Bremen, Germany) with the following settings: Full scan range 350–1600 *m/z*, max. 9 MS2 scans (activation type CID), repeat count 1, repeat duration 30 s, exclusion list size 500, exclusion duration 60 s, charge state screening enabled with rejection of unassigned and +1 charge states, minimum signal threshold 10,000.

2.3.6. Protein identification and label free quantification

P. sativum remains to be sparsely sequenced because of repetitive DNA that complicates a shotgun proteomic approach. Thus a database (db) was assembled according to [51] with minor modifications: UniProt UniRef100 db (22 January 2015) were sourced from the following taxa: *P. sativum*, *R. leguminosarum*, *Glomus*, and *Mycosphaerella*. Because of little entries for *P. sativum* at UniProt, we included organism specific sequences from NCBI. Additionally, assembled ESTs of *P. sativum* were sourced from www.coolseasonfoodlegume.org (unigene v2, unigene) [49] and subsequently six-frame-translated using mEMBOSS v6.5. The longest continuous amino acid sequence (longest open reading frame) within forward and reverse translation was chosen. Protein annotations were derived via BLAST against the complete UniRef100 db. Specific blast information was provided in brackets in the protein description (UniRef100 accession, identical coverage, query coverage, e-value). The identical sequences and subfragments were placed into a single record to avoid redundancy. The db was finally completed with cultivar specific mutations according to [51] and comprised 140,560 entries.

Thermo raw files were identified and quantified in MaxQuant [52]. Identification parameters were adapted to the respective instrument (Orbitrap Elite/Orbitrap XL): first search peptide tolerance 20 ppm/20 ppm, main search tolerance 4.5 ppm/6 ppm, ITMS MS/MS match tolerance 0.8 Da/0.8 Da, intensity threshold 500/500. All files were searched with maximum 5 of the following variable modifications: oxidation of methionine and acetylation of the N-term. Maximum two missed cleavages were allowed. A retention time window of 20 min was used to search for the best alignment function and identifications were matched between runs in a window of 0.7 min. A revert decoy db was used to set a cut-off at a FDR of 0.01 (at PSM and protein level). A minimum of 6 amino acids was required for identification of a peptide and at least two peptides necessary for protein identification. Label free quantification (LFQ) was done when at least one MS2 scan was present. LFQ minimum ratio was set to 2. Stabilisation of large LFQ ratios was active.

2.4. Statistical analysis

A two-way ANOVA was used to examine the main effects and interaction of biotic stress (with/without *D. pinodes* infection), and NP nutrient sources (microbial symbionts or mineral fertilizer) on shoot green area, shoot dry matter yield, root AMF colonisation and rhizobial nodulation. All assumptions required by ANOVA were verified. Differences between treatments were compared with Tukey's multiple range test, and statistical significance was defined at $P < 0.05$. These analyses were performed using SAS v. 9.4.

In proteomic and metabolomic studies, all statistical computation was done in R [53]. Outliers (1.5 times the interquartile range) of protein and metabolite intensities) were removed. Only proteins/metabolites present in more than half of the observations of a group were considered for statistical analysis. If less than half of the observations in a group were missing, the missing values were estimated via k-nearest neighbour algorithm. Remaining missing values were filled with half the minimum value of the respective protein/metabolite. Significant differences between groups were determined with an ANOVA followed by a Post-hoc test (Tukey HSD, $P < 0.05$). Significant proteins additionally required a minimum fold change of ≥2.

The average intensity of statistically significant proteins among healthy treatments was scaled (*z*-transformation). Proteins were hierarchically clustered with Euclidian distance and complete linkage method and plotted with heatmap.2 function [54] and 'YlOrRd' colour palette from the 'RColorBrewer' package [55]. The proteins were functionally classified with Mercator [56], filtered to the most representative functions (only proteins with assigned function; minimum count of 4 proteins per function) and visualised in a stacked bar plot (Fig. 7B). Proteins/metabolites significantly responding to disease were determined via a comparison (ANOVA, Tukey HSD) of the diseased versus the healthy plants (e.g. Md/Mh) and a comparison (Student's *t*-test) of all diseased versus healthy plants (d/h). Corrected *p*-values (Benjamini Hochberg) are additionally provided.

The scaled protein averages were clustered and plotted in a heatmap. Stress related categories were visualised as well as responsive categories with >4 proteins per functional category. Averages of metabolite intensities were used to calculate the ratios between diseased and healthy treatments. The ratios are visualised with the 'RdBu' colour palette (RColorBrewer package). Pathway visualisation was adopted from Schweiger et al. [24].

3. Results

3.1. Phenotypic characterisation

For the determination of symbiont root colonisation and its effect on pathogen disease severity as well as on plant growth, several analyses where carried out at the stipules, leaflets and roots with the following results:

3.1.1. Disease severity

We noted significant difference in disease development between two scoring dates of disease severity (DS) on both stipules and leaflets, but not among symbiotic treatments. After nine days of pathogen

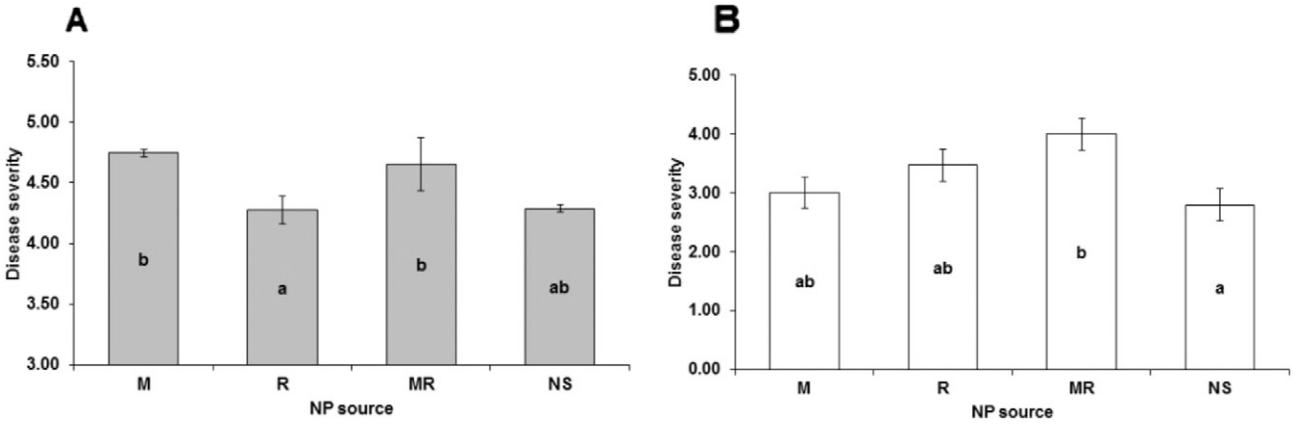

Fig. 1. Effects of absent, dual or tripartite symbiosis with arbuscular mycorrhizal fungi (AMF) and/or *Rhizobium leguminosarum* bv. *viceae* on pathogenic disease severity of *P. sativum*: leaflets (A) and stipules (B) nine days after infection of *D. pinodes*. Abbreviations are: M (AMF); R (*Rhizobium* bacteria); MR (dual M and R); NS (non-symbiotic synthetic dual nitrogen and phosphorus fertilizers). Values are means ($n = 4$) and error bars indicate standard error. Bars labelled with the same letter are not significantly different from each other according to Tukey's HSD at $p < 0.05$.

infection, however, the mean DS on leaflets of plants inoculated with single R was significantly lower than on plants with AMF treatment (M and MR). This effect of Rhizobia on the disease severity was not found on stipules (Fig. 1A, B). The overall DS ranged from 2.3 to 4.5 on the leaflets and from 0.4 to 3.2 on the stipules between the two scoring dates. The DS range was much smaller on leaflets than on stipules, however, DS was higher. Possibly leaflets were most accessible to the spray of spores that led to rapid disease progress and higher initial DS score. A general downward (not upward) disease progress from leaflets to petioles, stipules and to the base of stems was noticed.

3.1.2. Mycorrhizal root colonisation

To assess the efficiency of dual and tripartite AMF associations with host plants under healthy conditions and *D. pinodes* attack, mycorrhizal root colonisation was measured. Healthy plants inoculated with single mycorrhiza (M) showed the maximum fungal root colonisation of 62% (Fig. 2). The biotic stress significantly reduced root mycorrhizal colonisation by 30% compared to healthy plants. Furthermore, antagonistic effects of dual MR inoculation were noted under both healthy and diseased plant growth conditions with a 13% to 15% reduction compared to single AMF inoculation, respectively. For control, random samples from plants without AMF inoculation never showed any AMF colonised roots.

3.1.3. Efficiency of root nodulation by rhizobia

To evaluate inoculation with *Rhizobium*, we determined nodule dry weight (DW) as well as number. Plants inoculated with single R had approximately 30% significantly higher nodule DW than co-inoculated (MR) plants (Fig. 3). The interaction between pathogen and *Rhizobium* inoculation showed significant effect on nodule DW both for treatments R and MR (Fig.3). Pathogen infection reduced nodule DW by 75%. Overall, nodule distribution and size were bigger and confined around the crown root, particularly in the single R system. As control, random samples from plants without *Rhizobium* inoculation never showed any nodule-like structures on the roots.

3.1.4. Green area production

A two-way ANOVA indicated that there were no statistically significant interaction effects between pathogen infection and symbiotic treatments on green area (GA) production (Fig. 4). However, about 80% GA reduction was found due to *D. pinodes* infection as compared to healthy pea plants. Independent of the treatment, in our experimental setup GA was only affected by plant health (e.g. Fig. S1).

3.1.5. Shoot dry matter production

To reveal the effects of biotic (pathogenic) stress and microbial symbionts' interactions on photosynthetic performance of plants, the dry weight (DM) of shoots was determined. Overall, the mean DM

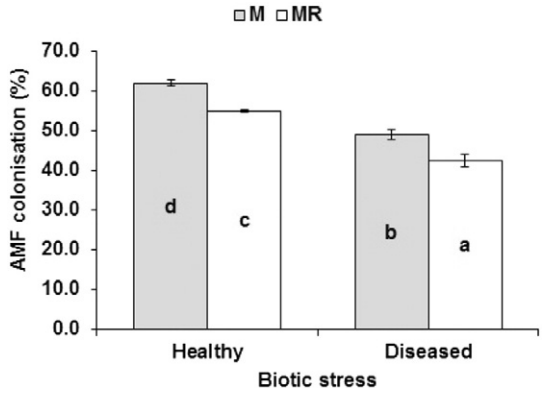

Fig. 2. Efficiency inoculation of field pea (*Pisum sativum* L.) with single AMF or combined with *Rhizobium* bacteria (MR) on mycorrhizal root colonisation under healthy and biotic (*D. pinodes*) stress plant growth conditions. Error bars indicate standard error ($n = 4$). Bars labelled with the same letter are not significantly different from each other according to Tukey's HSD at $p < 0.05$.

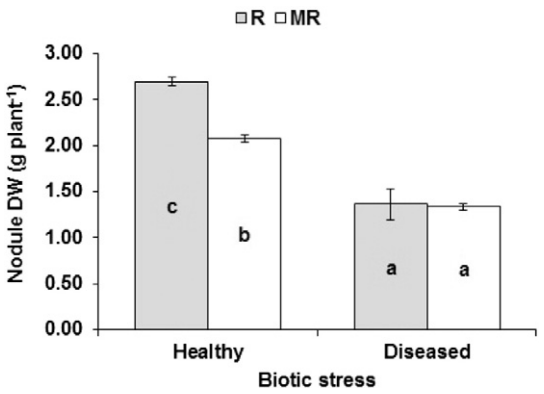

Fig. 3. Efficiency of inoculation of field pea (*Pisum sativum* L.) with single *Rhizobium* bacteria (R) or combined with AM fungal (MR) on root nodule dry weight (DW) under healthy and biotic (*D. pinodes*) stress plant growth conditions. Error bars indicate standard error ($n = 4$). Bars labelled with the same letter are not significantly different from each other according to Tukey's HSD at $p < 0.05$.

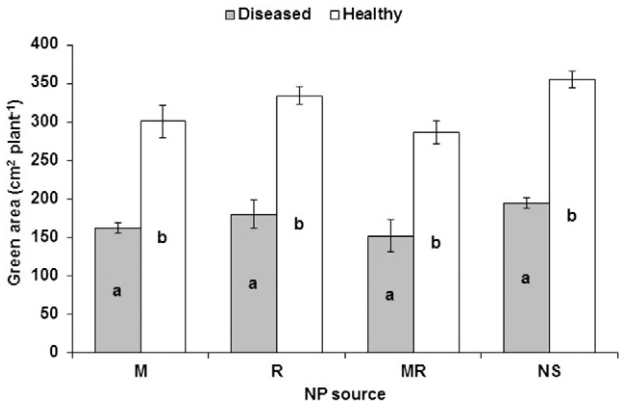

Fig. 4. Effects of NP sources from microbial symbionts and synthetic fertilizers on green area production of field pea (*Pisum sativum* L.) under healthy and diseased plant growth conditions. Abbreviations are: M (AMF); R (*Rhizobium* bacteria); MR (dual AMF and R); NS (non-symbiotic synthetic dual nitrogen and phosphorus fertilizers). Values are means ($n = 4$) and error bars indicate standard error. Bars labelled with the same letter are not significantly different from each other according to Tukey's HSD at $p < 0.05$.

production was significantly lower in diseased plants than in healthy ones by 70% (Fig. 5). DM was also found to be partly treatment specific. The R treatment showed significantly higher mean shoot DM of healthy and diseased plants (2.4 g pot^{-1}) compared to M with lowest mean DM production of 1.8 g pot^{-1}. Again, statistically significant interaction effects between pathogen infection and treatments were found.

3.2. Integrative molecular and subcellular analyses of the proteome and metabolome

For the investigation of the molecular effects of the different symbiotic treatments and their possible influence on the plants leaflet response to the pathogen attack, an integrative proteome and metabolome extraction as well as an additional subcellular proteome extraction of the cytosol and the plasma membrane were performed. For best data presentation, we decided to combine quantitative proteomics data of the integrative and cytosolic extractions separately from plasma membrane proteins and metabolites.

3.2.1. Functional and local proteome characterisation

Altogether, 1564 proteins were used for quantitative analysis. Because of the largest complexity the integrative leaf extracts accounted for the majority of identifications (1383; Fig. 6) including especially

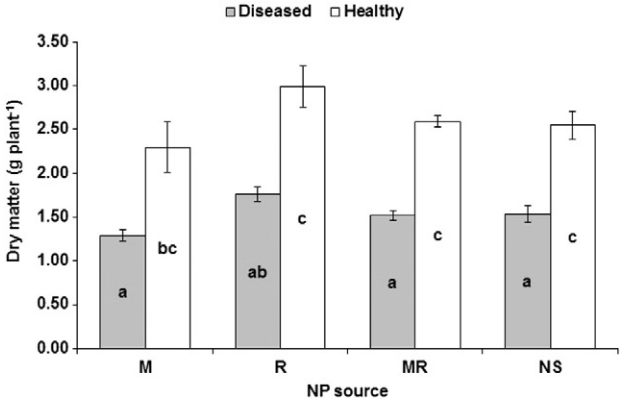

Fig. 5. Effects of NP sources from microbial symbionts and synthetic fertilizers on dry matter production of field pea (*Pisum sativum* L.) under healthy and diseased plant growth conditions. Abbreviations are: M (AMF); R (*Rhizobium* bacteria); MR (dual AM fungi and R); NS (non-symbiotic synthetic dual nitrogen and phosphorus mineral fertilizers). Values are means ($n = 4$) and error bars indicate standard error. Bars labelled with the same letter are not significantly different from each other according to Tukey's HSD at $p < 0.05$.

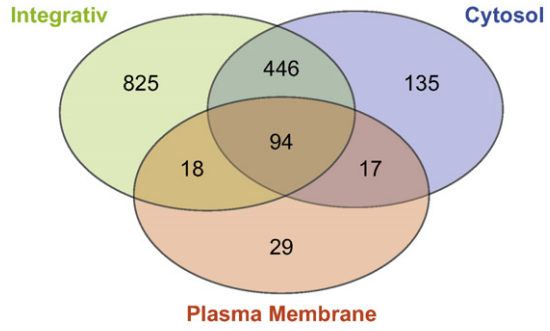

Fig. 6. Number of quantified leaf proteins from total integrative extraction, cytosolic fraction and plasma membrane enrichment.

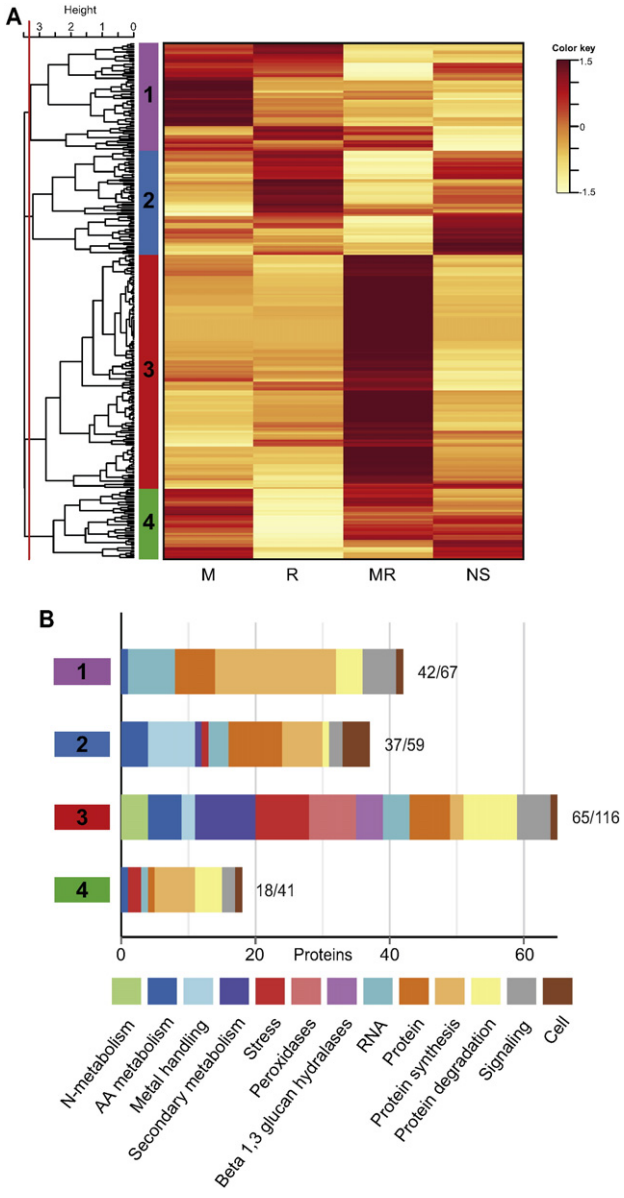

Fig. 7. (A) Heatmap of 293 protein abundances from the integrative and cytosolic extraction which showed a significant difference among symbiont treatments of healthy plants. Each cell represents the scaled average protein intensities ($n = 3$). Euclidean distance and complete linkage method were used for cluster analysis. Clusters (1–4) were grouped at a height of 3.3; (B) clusters from (A) were functionally categorized by adopting functional bins from the MapMan Mercator tool. Categories were plotted when containing a minimum of 4 proteins in at least one cluster. Values at the bars' right side represent the number of categorized proteins per number of proteins in the corresponding cluster (1–4) derived from (A).

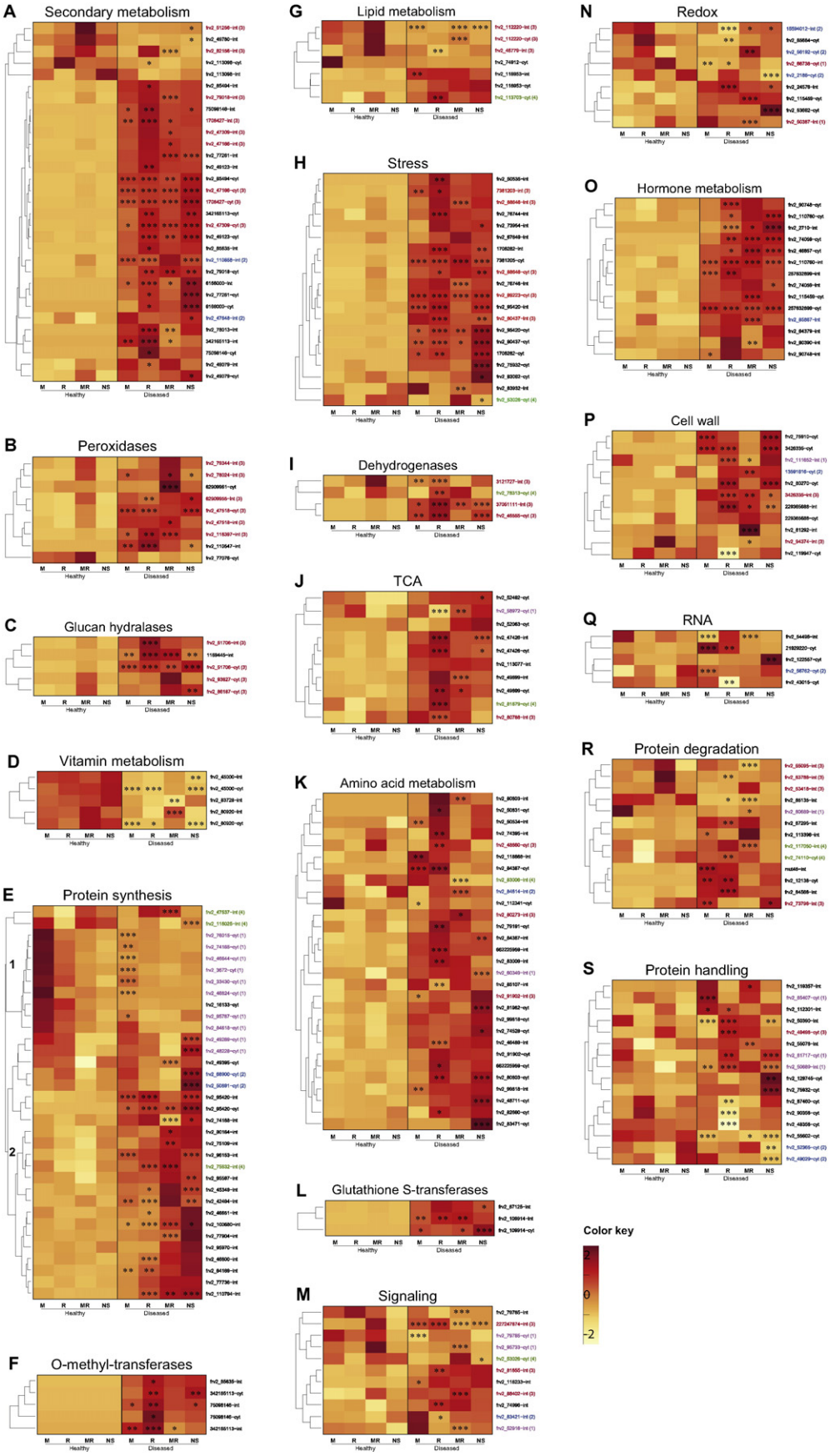

Fig. 8. (A–S) Heatmaps of functionally annotated proteins that significantly changed upon infection; exclusively proteins with known function and a minimum of 4 proteins per category were hierarchically clustered (Euclidean distance, complete linkage). Protein accessions also found significant among healthy plants (Fig. 7) are colour coded and marked with the respective cluster number. Asterisks indicate *p*-values of treatment response to infection: $^{*}p < 0.05$, $^{**}p < 0.01$, $^{***}p < 0.001$.

the plastidic proteome with the most abundant proteins of the photosynthetic apparatus (e.g. Calvin Cycle). The additional subcellular enrichment of the cytosol (692) and the plasma membrane (158) fractions, lead to the quantification and localisation of additional 135 and 29 proteins, respectively (Fig. 6). Many of those proteins provided additional information especially to amino acid metabolism, protein synthesis and protein handling, which were also involved in pathogen response (Fig. 8N and C). Cytosolic proteins mostly overlap with integrative extracted proteins, whereas identifications of the plasma membrane overlap likewise with both integrative and cytosolic fractions.

By using the agriGO tool (v. 1.2) [57], the cellular compartment was predicted for all identifications of the plasma membrane purified fraction. Supplementary Fig. S2 indicates that a good portion (39/135) of these identifications was related to the plasma membrane but also to the cytoplasm. On one hand, this means that several plasma membrane proteins where also found in the integrative and cytosolic extractions and some proteins of unknown annotation may possibly be associated with the plasma membrane. On the other hand, several proteins might be derived from expected contaminations mainly of the cytosol due to incomplete purification [58]. In the following accessions of significantly responding proteins these are marked with -int (integrative extraction only) or -cyt (cytosolic extraction only) or -int-cyt (from both extractions), depending on where these have been found.

3.2.2. Symbiont treatment effect on proteome and metabolome of healthy plants

A heatmap was generated with all 293 proteins of the integrative and cytosolic extraction, significantly different in abundances between treatments of the healthy plants (Table S2; $p < 0.05$, fold change ≥2) (Fig. 7A). The intensity values for label free quantification were used for hierarchical cluster analysis. Four treatment specific clusters (cluster height 3.3) were further functionally grouped (Fig. 7B).

The first set (violet) represents proteins with elevated abundance in R and specifically in M treated plants (Fig. 7A). To a high degree these proteins are involved in RNA and protein metabolism (Table S2; protein targeting, post translational modifications, synthesis, and degradation). The second set (blue) with highest levels in R and NS treatments includes a large part of metal handling proteins (mostly ferritins: frv2_45286-int-cyt, frv2_45302-int-cyt, frv2_74959-int) as well as proteins involved in protein regulation. However, MR plants showed by far the largest set (116 proteins — red) which mainly consisted of proteins categorized in, or related to stress response (secondary metabolism, Fig. 8A; beta 1,3 peroxidases, Fig. 8B; glucan hydralases, Fig. 8C). The majority of those proteins involved in secondary metabolism belonged to flavonoid synthesis (e.g. chalcone–flavanone isomerase, isoflavone reductase). The functional category signalling noteworthy comprises more proteins in sets with high abundance in symbiotic treatments (violet, red), but not in the NS ones (blue, green).

Differences were observed in 15 metabolites among healthy plants that are explained by two main observations: (1) Elevated levels of glutamine and oxaloacetate and lower levels of leucine in NS plants; (2) high levels of galactinol, galactose, isoleucine, phenylalanine, valine, threonine, asparagine, benzoate, butanoic acid, nicotinic acid and butyro-1,4-lactam in MR plants (Table S2). In healthy plants, we observed significantly higher abundance of γ-aminobutyric acid (GABA) in M than in R.

3.2.3. Effect of pathogen infection on the plant proteome and primary metabolism

With this proteomic approach a quantity of 301 proteins were found to change abundance upon infection (Table S3).

Proteins from the plasma membrane extract were exclusively compared on the infection level as a consequence of too little observations caused by low protein yield in samples of specific treatments (MR, R). All 11 proteins that were found significantly responding to infection were accumulating (Table 1). About half of the proteins responding upon infection in the plasma membrane were also found to be induced in the integrative and cytosolic samples. Among them was the disease resistance response protein Pi49 (PR10 like), which showed the highest fold change in the plasma membrane fraction.

The following proteins were solely found significantly upregulated upon infection in the plasma membrane fraction but not in the cytosolic or the integrative extraction: V-type H^+-ATPase subunit β (frv2_111907), translational elongation factor 1 subunit β (frv2_75243), PfkB family carbohydrate kinase (frv2_83550), and proteasome subunit β (frv2_86875).

Abundances of proteins which showed response to the infection (including some proteins that contributed to significant differences among healthy treatments) were grouped according to their function and visualised in cluster heatmaps (Fig. 8; functional clusters A–S). All proteins with information about ratios and *p*-values can be found in Table S3.

Only proteins of the categories vitamin metabolism (Fig. 8D) and few proteins of the secondary metabolism (Fig. 8A) as well as from protein synthesis (Fig. 8E) were substantially depleted upon pathogen infection. In vitamin metabolism (Fig. 8D), phosphomethylpyrimidin synthase (frv2_80920-int-cyt), thiamine thiazole synthase (frv2_45000-int, frv2_45000-cyt) as well as its possible reaction centre (frv2_83728-int) were significantly reduced upon infection. This oxidative stress upon infection is as well reflected in the higher levels of SOD (frv2_85684-cyt; redox).

Overall, most functional categories reveal a substantial protein accumulation upon infection. We found an isoflavone-7-*O*-methyltransferase (frv2_85635-int) and two isoforms of the (+)-6a-hydroxymaackiain 3-*O*-methyltransferase 1/2 (342165113-int-cyt, 75098146-int-cyt) to be induced exclusively at disease response (Fig. 8F; *O*-methyl-transferases).

Noticeable, the single rhizobia inoculated plants showed the most significant response of all treatments in the pisatin pathway. Upstream the flavonoid synthesis, we also found that 2-hydroxyisoflavanone dehydratase (frv2_118953-int-cyt; Fig. 8G; lipid metabolism) was exclusively upregulated in diseased plants.

Stress related proteins were similarly induced independent of the symbiotic treatments, whereas certain subsets (Fig. 8H; accessions indicated red; PR proteins, endochitinases) showed high abundance also in healthy co-inoculated (MR) plants. This applies also for proteins related to secondary metabolism, peroxidases and dehydrogenases (Fig. 8A, B and I). However, such difference was not observed among infected treatments, where R and/or NS plants seemed to show the strongest response in abundance (Fig. 8F, J and K; *O*-methyl-transferases, TCA, amino acid).

Glutathione-*S*-transferases (Fig. 8L), which are catalysing the binding of glutathione to Xenobiotics, were exclusively upregulated in diseased plants. Glutathione synthesis requires the amino acid glycine, which was mainly downregulated (Fig. 9), while glutamate and cysteine showed no significant regulation. Proteins attributed to signalling function show diverse characteristics among healthy, as well as diseased plants (Fig. 8M).

Plants inoculated with rhizobia exhibited high levels of thioredoxin (15594012-int, frv2_56192-cyt) and superoxide dismutase (SOD; frv2_85684-cyt) which were downregulated upon disease, whereas other treatments responded contrary (Fig. 8N; redox). Despite this rhizobial dominated priming, we also noted a common upregulation of redox associated proteins (Fig. 8N) in disulphide isomerases (frv2_24576-int, frv2_53662-cyt), and 1-aminocyclopropane-1-carboxylate oxidase (frv2_115459-cyt). Upstream, methionine is processed to *S*-adenosyl-L-methionine via *S*-adenosylmethionine synthase to 1-aminocyclopropane-1-carboxylate. We observed that several isoforms of the *S*-adenosylmethionine synthase (Fig. 8K and O) involved in amino acid and hormone metabolism (frv2_46489-int, frv2_46489-cyt, frv2_74528-int, frv2_74528-cyt, frv2_99818-cyt, frv2_46489-int, frv2_74528-int) were significantly

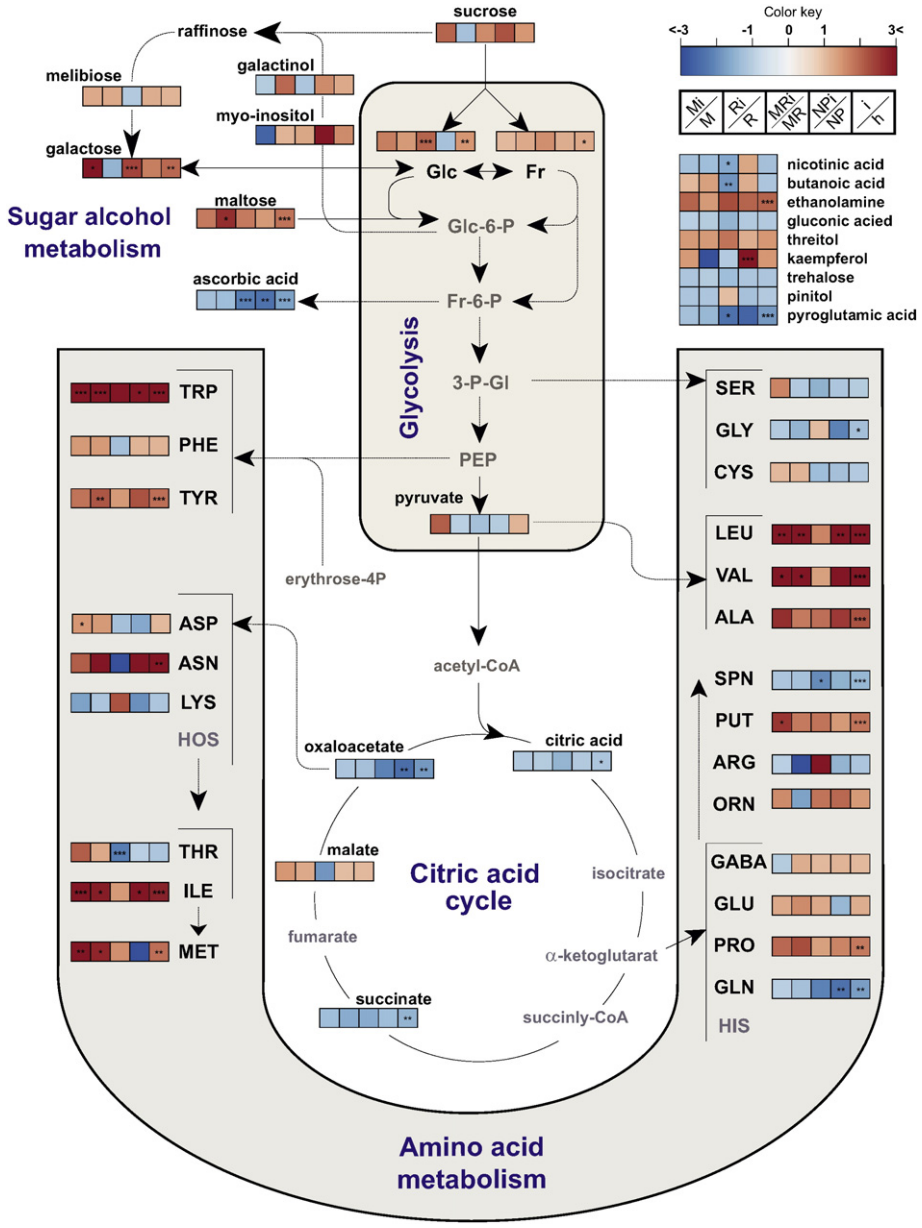

Fig. 9. Schematic overview of the primary metabolism: Metabolite levels of different symbiotic treatments that significantly changed upon infection (blue: decrease, red: increase); i = infected; h = healthy; Asterisks indicate *p*-values: $^{*}p < 0.05$, $^{**}p < 0.01$, $^{***}p < 0.001$.

upregulated upon infection. Furthermore, ascorbate and methionine pools showed notable changes in diseased plants: In M and R treatments with increased methionine, there was no significant decrease in ascorbate. In contrast, MR and NS treatments with no significant increase in methionine showed a significantly depleted ascorbate pool.

Fig. 8O indicates hormone metabolism, besides, ET and SA (acyl-[acyl-carrier-protein] desaturase, frv2_113703-cyt) responding pathway proteins, a set of two isoforms of 12-oxophytodienoate reductases (frv2_110760-int, frv2_110760-cyt, 257632899-int, 257632899-cyt), belonging to the jasmonate (JA) synthesis pathway showed increased abundance in all diseased plants.

Fig. 8P shows the cell wall metabolism that responded with increased levels of pectin esterases (3426335-int-cyt, frv2_80270-cyt) as well as UDP-D-glucuronate carboxy-lyase (13591616-int-cyt) and UDP-glucose 4-epimerase (229365688-int). Additionally, a leucine rich repeat showed response especially in diseased M and NS plants.

The three initial enzymes of the citric acid cycle (Fig. 8J; TCA), citrate synthase (frv2_113077-int), aconitase (frv2_52492-cyt/int), isocitrate dehydrogenase (frv2_81879-int-cyt), and also succinyltransferase (frv2_52063-cyt) were upregulated in all treatments, although R showed the most significant response. Similarly, amino acid metabolism (Fig. 8K) was mostly affected in rhizobial plants upon infection.

Metabolites, participating in the TCA (Fig. 9), such as citric acid, succinate, and oxaloacetate, showed exclusively lower levels in diseased plants than in healthy ones, except for malate which was similar in both of them.

RNA regulation (Fig. 8Q) and protein synthesis (Fig. 8E) comprises a large part of the infection response. In protein synthesis 2 subclusters can be distinguished. A remarkable set (subcluster E1), mainly ribosomal proteins (coloured violet; high in M) was exclusively depleted in M plants upon infection. However, the most common infection response (subcluster E2) consisted of an accumulation especially of ribosomal

proteins and EF2. Moreover, proteins involved in protein folding were significantly accumulating mainly in NS and R infected treatments.

A subset of proteins involved in protein degradation (Fig. 8R; frv2_53418-int, frv2_65095-int, frv2_83788-int) was specifically high in MR plants but levelled out in diseased plants. Proteins involved in protein folding, protein targeting or posttranslational modifications are combined in the functional group protein handling (Fig. 8S) which mostly comprises of chaperones (frv2_129745-cyt, frv2_81717-cyt), peptidyl-prolyl *cis*-trans isomerases (frv2_87460-cyt, frv2_50390-int), a heat shock protein (frv2_75932-cyt) and a patellin-2-like protein (frv2_49029-cyt). The majority of proteins in this category were found in the cytosol.

The infection affected 28 primary metabolites (Table S3) being visualised in Fig. 9. Briefly, among sugars, glucose and fructose were accumulated. Interestingly, we also noted a concomitant increase of several amino acids such as tryptophan, tyrosine, isoleucine, methionine, leucine, valine, alanine, and proline. Here, homoserine was poorly quantified. However, metabolic precursors for HOS (aspartate, asparagine) and its derivatives (isoleucine, methionine) were significantly upregulated (Fig. 9; amino acid metabolism). Co-inoculated plants (MR) showed eased or contrary response in these amino acids.

4. Discussion

This is, so far, the most comprehensive study of proteome and metabolome infection response to *D. pinodes* [48,59].

The main goal of our study was to reveal whether and how the different microbial treatments effect on plants metabolism and growth performance (4.1) and whether and how this would influence susceptibility of *P. sativum*'s response to the pathogenic induced ascochyta blight by *D. pinodes* (4.2). Differential symbiont treatments showed distinct effects on the plant metabolism with only little impact on growth as reflected by green area and dry matter production. But infected plants were strongly injured by the fungal disease.

4.1. Differential symbiont treatments show distinct effects on the plant metabolism with only little impact on the plants green area and dry matter production

Green area of pea plants depends on the addition and expansion of new leaves, pods or stem tissue and the senesences of older, dying leaves and maturing pods. Generally, the phenotypic host plant benefits in green area and dry matter production obtained from each microbial symbiont were sufficient and similar to the non-symbiotic treatment with synthetic fertilizer. As previously reported, metabolic exchanges from the microbial symbionts for host C have a stimulatory effect on leaf photosynthetic capacity [30], enhance green area growth and may also trigger systemic induced resistance against stress [12,60].

Plants inoculated with single AMF, however, showed mildly decreased dry matter compared to the other treatments. The distinct leaflet-proteome patterns that we found in response to different symbiotic treatments of *P. sativum* seemed, however, only slightly involved in growth performance. The AMF specific protein pattern was specifically striking for its higher levels of several proteins involved in protein regulation and synthesis. However, there was no clear indication of this AMF specific protein pattern to negatively regulate plant growth performance.

At least, the slightly enhanced dry matter of rhizobia treated plants matched well with the distinct accumulation of proteins involved in cell regulation such as tubulins (Fig. 7B; cell). Our results show that protein synthesis and RNA related proteins were dominant in the proteome of healthy plants inoculated with single rhizobia or AMF, but not with combined MR or synthetic fertilizer (NS). Among them the nascent polypeptide-associated complex subunit β was of great abundance. As reviewed by Rospert et al. [61], the nascent polypeptide-associated complex was suggested to shield nascent polypeptides deriving from the ribosome, and to be a negative regulator for translocation into the endoplasmic reticulum, but a positive one for translocation to the mitochondria. In addition, this complex was proposed to play a role in transcription rather than translation. Transcriptional changes were previously suggested to be highly controlled by the process of autoregulation of mycorrhisation or nodulation in *Glycine max* [62]. The higher levels of nascent polypeptide-associated complex subunit beta were accompanied by upregulation of a translation elongation factor-2 subunit in plants inoculated with single microbial symbionts. That is in agreement with Staudinger et al. [49], where rhizobia inoculated *Medicago truncatula* plants exhibited higher levels of elongation factor-2.

The tripartite association (MR) failed to show its synergistic effects on maximising both green area and dry matter production over the individual microbial symbionts (M or R). That might be mainly attributed to the lower effectiveness of the AMF symbiosis. A reduction of mycorrhizal benefit to host plants with increasing plant density has been reported by [63,64]. Furthermore, such lower root colonisation and nodulation in a combined MR situation might be attributed to competition between them for survival and multiplication, energy (C), nutrients and space on roots [65,66]. Nevertheless, the antagonistic effect that leads to lower colonisation observed for AMF and rhizobia of MR treated plants are consistent with other studies [32,37]. Similar results were reported previously, where AMF infection rate was lower in the tripartite symbiosis, but the number of nodules was not altered, however, nitrogenase activity was depressed [67]. A possible inhibition of N fixation and a negative effect on nodule development due to AMF colonisation of root nodules were reported [36–38]. Hence, our MR treatment results are in agreement with previous studies [32,37], but also contradicted others [68,69] which reported synergistic effects. The combination and efficiency of symbionts on plant species or even cultivars may be involved in the different findings.

It remains to be clarified, if this antagonistic effect is somehow linked to the distinct tripartite leaf-proteome pattern. Here, compared to the other treatments, the large number of highly accumulated proteins of the nitrogen- and secondary metabolism, stress, peroxidases and beta 1,3 glucan-hydratases pathways may be noticeable. These pathways are well known to be involved in stress response.

For instance, we found 12-oxophytodienoate reductase (frv2_110760) significantly higher (1.5 fold) exclusively in healthy tripartite plants compared to other treatments (M, R, NS). The 12-oxophytodienoate reductase catalyses the penultimate step in the JA synthesis. JA biosynthesis is known to be induced in barley [70] as well as in leaves of tomato associated with AMF [71]. Furthermore, a hypernodulating mutant of *Glycine* was shown to exhibit elevated levels of JA in the leaves indicating that this phytohormone is involved in the autoregulation of nodulation [72,73]. Others indicated that the degree of mycorrhisation reduces with lower levels of JA [74], which suggests a mediation of the plant–fungus interaction by this hormone. Kiers et al. [75] found that low levels of exogenously applied JA positively affect AMF colonisation, whereas high levels impede its colonisation. The suppressing characteristic of JA was recently affirmed in the interaction of *Populus* and *Laccaria bicolor* [76]. We also observed high abundance of metabolites and proteins related to flavonoid synthesis (phenylalanine, chalcone synthase/isomerase, isoflavon reductase) in MR treated plants that might play a role in the synthesis of Pisatin, the major phytoalexin in pea, known to be induced upon *D. pinodes* infection [77]. Changes in the composition of flavonoids in the shoot upon association with AMF were observed earlier in *Trifolium repens* [78]. In accordance with other studies, where glucan hydralases were found to be induced upon metal stress and JA signalling [79,80], we also observed high abundance of these proteins in MR plants.

We found a remarkable similarity between the induction of peroxidases of the tripartite treatment (MR) and the known general stress response mechanism in various plant species [81–83]. In MR plants, an accumulation of monodehydroascorbate reductase was observed, while their ascorbate level was equivalent to M, R and NS treatments.

This suggests that the glutathione ascorbate cycle is more active in tripartite plants and leads to the assumption that these peroxidases are mainly inactivating H_2O_2 within the cell by utilizing NAD(P)H. This is supported by the elevated levels of nicotinate, which serves as pyridine precursor [84] and mediates NAD synthesis [85]. It was proposed previously that enhanced resistance is accompanied by an increase of NAD, but not of ascorbate or glutathione in the leaves [86]. The demand for reduction equivalents can be affirmed by our observation of significantly increased *S*-(hydroxymethyl)-glutathione dehydrogenase, responsible for reduction of $NAD(P)^+$ to NAD(P)H, as well as the high abundance of phosphogluconate dehydrogenase and chloroplastic ferredoxin NADP oxidoreductase (Table S3) that both participate in the oxidative pentose pathway (OPP) providing NADPH. Our results suggest that aside the OPP, additional NADPH is produced through the Hatch-Slack pathway commonly known as C_4 photosynthesis.

Concerning microbial induced systemic stress alleviation, the proteomics data show further interesting overlaps with previous studies. In both, the single AMF and rhizobia treatments leaves showed an induction of metal handling proteins.

Heavy metal uptake and translocation was reported to be lower in mycorrhiza associated plants [87,88]. Even though the sets of induced metal binding proteins are different between the two symbiont treatments, in future it will be interesting to study if these are also involved in heavy metal stress alleviation for R treated plants. AMF protects plants against oxidative stress caused by heavy metals in the soil as reviewed by Schutzendubel and Polle [89]. Other authors thereon suggested a decreased need for reactive oxygen species (ROS) scavenging mechanisms in the shoot [79] and found, among other proteins, *S*-adenosylmethionine synthase (SAMS) downregulated in AMF associated plants (Table S3). *S*-adenosylmethionine (SAM) is a precursor of nicotianamine, which has been reported to play a role in metal ion homeostasis through chelation mechanisms and transport [90,91]. SAM additionally serves as a substrate for certain methylases regenerating glutathione (GSH) via the GSH-ascorbate-cycle.

In accordance to this, in tripartite (MR) plants, we found low levels of SAMS and aci-reductone dioxygenase (1,2-dihydroxy-3-keto-5-methylthiopentene), involved in methionine salvage. Affirmative to this, MR treated plants exhibited low ferritin pools, which are reported to protect cells against oxidative damage [92]. Altogether, these findings suggest a low demand for ROS scavenging mechanisms in mycorrhiza associated plants. However, the set of significantly altered proteins and metabolites (monodehydroascorbate reductase, peroxidases, galactose, nicotinate) in MR plants contradicts the assumption of lower activity in the ROS quenching machinery.

Overall, the relatively small number of proteins specifically accumulating in non-symbiotic plants emphasize significant microbial induced systemic leaf response to the symbiotic treatments as described previously [49,79,93].

4.2. Upon D. pinodes infection, a common pathogen response pattern is induced that superimposes most of the symbiont-acquired molecular response pattern

Infection and disease development depends on primary inoculum and on weather conditions which were optimum in this study. Consequently, our disease scores were similar to various previous studies such as [7]. We noted the severely negative effects of biotic (*D. pinodes*) stress on various aspects of plant growth such as green area and dry matter production as well as root nodulation and mycorrhizal colonisation. We also observed substantial changes in the composition of the proteome and metabolome.

The plasma membrane has been reported to play a key role in plants initial steps of defence signalling against pathogens [94]. The enrichment of the plasma membrane was satisfactory as suggested by an increased number of plasma membrane related proteins (Fig. S2). The greatest change upon pathogen infection was observed in the well characterized defence marker disease resistance protein Pi49 (PR10 like) [95,96], which is known to be induced by *D. pinodes* [97] and other pathogens [98] as well as by AMF and rhizobial symbionts [99].

Among proteins solely detected in the plasma membrane, a V-type H^+-ATPase subunit β was pathogen induced. This is well supported by the findings that plasma membrane H^+-ATPase are regulated by cytosolic Ca^{2+} [100] or bacterial pathogens [101]. The regulation of protein turnover upon pathogen infection [102] was also reflected in our results by upregulation of the proteasome subunit β, involved in protein degradation. Likewise, the *Arabidopsis* homologue (At5g19510) of the translational elongation factor 1 subunit β and a PfkB family carbohydrate kinase (At2g31390) were described to be responsive to bacterial pathogens and are confirmed to be localized in the plasma membrane (GO-annotation). Despite the relatively low yield of the plasma membrane fraction these proteins are evidenced key players and thus good marker proteins for plasma membrane localisation and pathogen attack. Nevertheless, further studies are necessary to clarify, if these markers are also involved in symbiont specific pathogen response or even improved pathogen resistance.

A common plant response against biotic stress was observed in the metabolome as well as in the proteome. Proline, which increased in diseased plants, was found to be induced by pathogen interaction triggering hypersensitive response [45,103] It is also known to be elevated upon environmental stress and reported to function in metal chelation, antioxidative defence as well as signalling [104].

We found that the primary metabolism contributes crucially to the plant's defence response in agreement with [25]. Above all, the TCA and amino acid metabolism (Fig. 8N and P) underwent fundamental regulations after pathogen infection. The most significant regulations in these pathways were present in rhizobial inoculated plants. The combined inoculated plants (MR), however, showed only minor response to infection (threonine, spermidine) what might be explained by the already affected concentrations in healthy MR plants. This applies also to certain functionally groups of proteins, which were elevated in MR plants, but levelled out in diseased plants (e.g. peroxidases, proteins associated to stress and secondary metabolism; Fig. 8B, I and A).

Upon pathogen infection, in all plants the TCA metabolites citric acid, succinate, and oxaloacetate exhibited low levels. This might derive from increased malate dehydrogenase synthesis, which was previously observed by Castillejo et al. [48] to be induced after *M. pinodes* infection. In all diseased plants, synthesis of PEPC was intensified. Exclusively in plants inoculated with rhizobia, increased levels of the NADP-dependent malic enzyme were observed. This indicates a need for stress alleviation. This enzyme was already shown to increase in *Pisum* upon infestation by *Fusarium oxysporum* [105]. The low levels of NADP-isocitrate dehydrogenase exhibited in R plants were significantly increased upon *M. pinodes* infection. This enzyme is mainly localized in the cytosol and was found to contribute to redox homeostasis and pathogen-response regulation in *Arabidopsis* [106].

There was an infection response in all treatments (M, R, MR, NS) in the ATP-citrate lyase which was emphasized in R and MR plants. ATP-citrate lyase was reported to be mainly localized in the cytosol and is responsible for the supply of Acetyl-Coenzyme A, which is required for the mevalonat pathway [107,108] and subsequently for isoprenoid synthesis. Isoprenoids are known to be produced upon fungal infection in rice [109]. However, our results showed a decrease of geranyl–geranyl diphosphate synthase (frv2_113098-cyt/int; Fig. 8C; secondary metabolism) in all diseased plants, which suggests a primary use of isoprenoids for gibberellin synthesis instead of higher terpenes. [110] reported higher resistance to the tobacco worm after silencing the geranyl-geranyl diphosphate synthase.

The importance of ROS is evident in the plant–pathogen interaction, which was expressed in our results via the upregulation of short chain dehydrogenases (SCD). Most of them are NAD(P) dependent oxidoreductases [111]. Short chain dehydrogenases are reported to regulate

PR1 gene expression in *Arabidopsis* [112] and thus mediate defence response.

At metabolite level, the change of redox balance was observed in the linkage of galactose, nicotinate and ascorbate which were affected by infection. The lower levels of ascorbate suggest its presence in oxidized form (dehydroascorbate, monodehydroascorbate), or utilized for example in ET synthesis. In treatments with upregulated methionine (M, R), ascorbate showed no significant decrease, whereas treatments with no significant change in methionine (MR, NS) showed a depleted ascorbate pool. Methionine is processed in the yang cycle, which is essential for ethylene synthesis. Thus our results indicate differential synthesis of ET solely in plants inoculated with single microbial symbionts (M or R).

As reported by Howe et al. [113], changes in the redox balance imply regulation of calmodulin dependent protein kinases and therefore signal triggering. In accordance to this, we found calmodulin, calnexin and other proteins exhibiting calcium binding EF-hand increased in diseased plants. Calcium signalling is known to regulate defence mechanisms in fungal interaction [114–116]. We found modulation of the hormone system corresponding to the observed signalling response.

The 12-oxophytodienoate reductase (JA synthesis), ACC (ET synthesis), S-adenosyl-L-methionine:salicylic acid carboxyl methyltransferase and acyl-[acyl-carrier-protein] desaturase (SA synthesis) were all upregulated upon infection. Indications of elevated JA synthesis (accumulation of lipoxygenases) upon symbiont treatments were observed. However there was no indication for symbiont induced SA or ET synthesis in healthy plants. With respect to pathogen attacks, it is important to know, that infection induces SA [117]. However, JA and SA pathways are known to antagonistically affect each other [118]. Thus, the elevated JA levels upon symbiont treatments may not play a beneficial role for pathogen defence as also previously described [71]. In agreement with our findings, they reported that AMF treated tomato plants showed increased lipoxygenase activity compared to non-symbiotic plants, but unlike with controls, this did not increase further in response to pathogen attack. Moreover, ET and JA are reported to act synergistically upon infection with necrotrophic pathogens [119] and suppress the abscisic acid (ABA) pathway [118].

Furthermore, it was reported that ABA positively mediates vitamin B_1 synthesis [120]. In agreement to this, the levels of phosphomethylpyrimidin synthase and thiamine-thiazole synthase, required for vitamin B_1 synthesis, were low. Consistent with other studies heat shock proteins and ABA-responsive proteins were upregulated upon infection [1]. ABA-responsive proteins are reported to have similarity to PR proteins which are as well induced upon stress [121]. Additionally, we observed an increase in all treatments in chaperones, PR-thaumatin proteins, chitinases, and disease resistance responsive proteins, which was accompanied by changes in the cell wall associated proteome (pectin methylesterases, β-xylosidase/alpha-L-arabinofuranosidase-like protein, UDP-glucose 4-epimerase, UDP-D-glucuronate carboxy-lyase, glycoside hydrolase and a leucin rich repeat protein), indicating modifications and reinforcement, as previously reported [43,122,123].

The largest set of increased proteins involved in secondary metabolism was mainly related to flavonoid synthesis (chalcone synthase, chalcone/flavonone isomerase, isoflavone reductase, sophorol reductase) and points directly towards pisatin synthesis. The (+)-6a-hydroxymaackiain 3-*O*-methyltransferase, processing the final step in the pisatin synthesis, was binned separately in the category *O*-methyltransferases (Fig. 8A). Nevertheless, pisatin is ineffective on pathogens such as *D. pinodes* as it is inactivated through pisatin demethylase, a cytochrome P450 [124].

Thereby it becomes visible that upon infection, the single rhizobia inoculated plants exhibited significantly greater abundance of this protein than M, MR and NS treated plants. This observation might be the major reason for the significantly lower level of disease severity compared to the other treatments. This higher abundance of pisatin pathway proteins fits to the greater response of the TCA and amino acid metabolism in rhizobial treated plants. Whether this rhizobial induced response was stronger or happened to occur sooner remains to be elucidated. Generally, a systemic resistance conferred by beneficial microbes is not associated with substantial alterations of the transcriptome [125] and plants are primed for enhanced defence. Thus, defence responses are not per se activated, but accelerated upon attack [126].

The crucial enzymes phosphoenolpyruvate carboxylase (PEPC) and NADP-dependent malic enzyme (ME) were both significantly accumulating in infected plants. This alternate pathway serves to alleviate abiotic stress via provision of CO_2 (to counteract oxygenase activity of Rubisco) and Pi through the PEPC [127], but also NADPH by the NADP-dependent ME. NADPH is needed for the antioxidant system and for biosynthesis of lipids, amino acids, and secondary metabolites. We found the latter two being upregulated in concentrations or activated in synthesis upon infection. Moreover, the PEPC replenishes intermediates of the TCA and subsequently scaffolds for amino acid synthesis. We confirm this by altered levels of TCA intermediates (↓oxaloacetate; ↑citric acid) and associated amino acids (↓asparagine; ↑aspartate, isoleucine, threonine, leucine, valine). Glutamine was also lower in all symbiotic compared to non-symbiotic plants. That was concomitant with elevated levels of glutamate decarboxylase and its product γ-aminobutyric acid (GABA). As reviewed by Shelp et al. [128], GABA synthesis is involved in nitrogen storage, plant development, defence, and acts as an alternative pathway for glutamate utilization. In addition, GABA is suggested to increase the efficiency of symbiotic N_2 fixation in legumes [129,130].

As discussed before, stress related proteins were strikingly abundant in MR plants suggesting a systemic induced defence response upon the tripartite interactions. Indeed, also pathogenic related stress response proteins like chitinases and PR-proteins were significantly increased. However, these proteins were only partially matched to those activated upon *D. pinodes* infection. It is known from *Arabidopsis* that certain chitinases are expressed in most of the organs at all growth stages [131]. Pathogenesis related (PR)-1 protein, which is reported to be a robust stress marker for salicylic acid (SA) responsive gene expression [118], was not increased in MR plants rather than PR-4 proteins. These were found to have a chitin binding domain [132] and antifungal activity in *Theobroma cacao* [133]. In *Arabidopsis*, PR-4 is also associated with the JA induced resistance against the necrotrophic fungus *A. brassicicola* [134]. The additional upregulated PR thaumatin family protein was reported to be induced similarly upon the incompatible interaction with wheat stripe rust (*Puccinia striiformis* f. sp. *tritici*, pathotype CY23) by JA [135].

5. Conclusions

There have been studies on the response of the *P. sativum* leaf proteome upon infection by *D. pinodes* but little is known about the effect of rhizobia and mycorrhiza on the leaf proteome and metabolome of healthy and diseased plants. Here, we found that root colonisation with symbiotic microorganisms (AMF and rhizobia) in bi- or tripartite association is able to satisfy plant N and P demand similar to synthetic fertilizer application, resulting in equivalent growth. Due to infection with the pathogen *D. pinodes*, plant growth is substantially impaired. Induction of symbiont specific molecular patterns in healthy leaves was characterized. Rhizobia or mycorrhiza inoculation severely affected leaf protein synthesis and RNA metabolism. Mycorrhizal inoculation also showed influence on metal handling and ROS quenching mechanisms. On the other hand, co-inoculated plants exhibited remarkable abundance of stress related proteins with a concomitant adjustment of proteins involved in jasmonate synthesis. The pathogen infection caused a common metabolic response (hormonal pathways, ROS scavenging, secondary metabolism and stress related proteins) that was more pronounced in rhizobial plants (TCA and amino acid metabolism, pisatin pathway), what concurred with fewer disease symptoms.

Hence, with this study we provide new insights into the symbionts induced systemic resistance of the leaf proteome as well as the specific early pathogen stress response, which emphasizes the importance of the plants interaction with microbial symbionts not only for nutrient acquisition. For further studies we suggest to compare cultivars in order to investigate different resistance levels derived from enhanced compatibility with symbionts.

Supplementary data to this article can be found online at http://dx.doi.org/10.1016/j.jprot.2016.03.018.

Transparency document

The Transparency document associated with this article can be found, in the online version.

Acknowledgement

The Austrian Science Fund (FWF) [P24870-B22] is gratefully acknowledged for the support of this work. We owe particular thanks to Diego Rubiales Olmedo and Mª Angeles Castillejo Sánchez for seed and pathogen supply. We are thankful to Rabea Schweiger for sharing graphical material for pathway visualisation. We thank Luis Recuenco-Muñoz for providing assistance with sampling. We also thank the gardeners Andreas Schröfl and Thomas Joch for plant cultivation at the department-associated greenhouse facility.

References

[1] S. Fondevilla, H. Kuster, F. Krajinski, J.I. Cubero, D. Rubiales, Identification of genes differentially expressed in a resistant reaction to *Mycosphaerella pinodes* in pea using microarray technology, BMC Genomics 12 (28) (2011) 1–15.
[2] B. Tivoli, S. Banniza, Comparison of the epidemiology of ascochyta blights on grain legumes, Eur. J. Plant Pathol. 119 (2007) 59–76.
[3] H. Ahmed, K.-F. Chang, S.-F. Hwang, H. Fu, Q. Zhou, S. Strelkov, et al., Morphological characterization of fungi associated with the ascochyta blight complex and pathogenic variability of *Mycosphaerella pinodes* on field pea crops in central Alberta, Crop J. 3 (2015) 10–18.
[4] T.W. Bretag, P.J. Keane, T.V. Price, The epidemiology and control of ascochyta blight in field peas: a review, Aust. J. Agric. Res. 57 (2006) 883–902.
[5] D. Shtienberg, Effects of foliar diseases on gas-exchange processes — a comparative-study, Phytopathology 82 (1992) 760–765.
[6] D.D. Bilgin, J.A. Zavala, J. Zhu, S.J. Clough, D.R. Ort, E.H. DeLucia, Biotic stress globally downregulates photosynthesis genes, Plant Cell Environ. 33 (2010) 1597–1613.
[7] G. Garry, M.H. Jeuffroy, B. Ney, B. Tivoli, Effects of Ascochyta blight (*Mycosphaerella pinodes*) on the photosynthesizing leaf area and the photosynthetic efficiency of the green leaf area of dried-pea (*Pisum sativum*), Plant Pathol. 47 (1998) 473–479.
[8] G.K. McDonald, D. Peck, Effects of crop rotation, residue retention and sowing time on the incidence and survival of ascochyta blight and its effect on grain yield of field peas (*Pisum sativum* L.), Field Crop Res. 111 (2009) 11–21.
[9] A. Schoeny, J. Menat, A. Darsonval, F. Rouault, S. Jumel, B. Tivoli, Effect of pea canopy architecture on splash dispersal of *Mycosphaerella pinodes* conidia, Plant Pathol. 57 (2008) 1073–1085.
[10] P. Jeffries, S. Gianinazzi, S. Perotto, K. Turnau, J.M. Barea, The contribution of arbuscular mycorrhizal fungi in sustainable maintenance of plant health and soil fertility, Biol. Fertil. Soils 37 (2003) 1–16.
[11] P. Sochacki, J.R. Ward, M.B. Cruzan, Consequences of mycorrhizal colonization for *Piriqueta* morphotypes under drought stress, Int. J. Plant Sci. 174 (2013) 65–73.
[12] D.K. Choudhary, A. Prakash, B.N. Johri, Induced systemic resistance (ISR) in plants: mechanism of action, Indian J. Microbiol. 47 (2007) 289–297.
[13] R. Ortiz-Castro, H.A. Contreras-Cornejo, L. Macias-Rodriguez, J. Lopez-Bucio, The role of microbial signals in plant growth and development, Plant Signal. Behav. 4 (2009) 701–712.
[14] K. Kosova, P. Vitamvas, I.T. Prasil, J. Renaut, Plant proteome changes under abiotic stress-contribution of proteomics studies to understanding plant stress response, J. Proteome 74 (2011) 1301–1322.
[15] F. Perez-Alfocea, M.E. Ghanem, A. Gomez-Cadenas, I.C. Dodd, Omics of root-to-shoot signaling under salt stress and water deficit, OMICS 15 (2011) 893–901.
[16] G.H. Salekdeh, S. Komatsu, Crop proteomics: aim at sustainable agriculture of tomorrow, Proteomics 7 (2007) 2976–2996.
[17] J.J. Calvete, Challenges and prospects of proteomics of non-model organisms, J. Proteome 105 (2014) 1–4.
[18] M.C. Romero-Rodriguez, J. Pascual, L. Valledor, J. Jorrin-Novo, Improving the quality of protein identification in non-model species. characterization of *Quercus ilex* seed and *Pinus radiata* needle proteomes by using SEQUEST and custom databases, J. Proteome 105 (2014) 85–91.
[19] J.V. Jorrin-Novo, J. Pascual, R. Sanchez-Lucas, M.C. Romero-Rodriguez, M.J. Rodriguez-Ortega, C. Lenz, et al., Fourteen years of plant proteomics reflected in Proteomics: moving from model species and 2DE-based approaches to orphan species and gel-free platforms, Proteomics 15 (2015) 1089–1112.
[20] J.V. Jorrin-Novo, Plant proteomics methods and protocols, Methods Mol. Biol. 1072 (2014) 3–13.
[21] T.D. Lodha, P. Hembram, N.T.J. Basak, Proteomics: a successful approach to understand the molecular mechanism of plant-pathogen interaction, Am. J. Plant Sci. 04 (2013) 1212–1226.
[22] F.M. Canovas, E. Dumas-Gaudot, G. Recorbet, J. Jorrin, H.P. Mock, M. Rossignol, Plant proteome analysis, Proteomics 4 (2004) 285–298.
[23] R.A. Dixon, D.R. Gang, A.J. Charlton, O. Fiehn, H.A. Kuiper, T.L. Reynolds, et al., Applications of metabolomics in agriculture, J. Agric. Food Chem. 54 (2006) 8984–8994.
[24] R. Schweiger, M.C. Baier, M. Persicke, C. Muller, High specificity in plant leaf metabolic responses to arbuscular mycorrhiza, Nat. Commun. 5 (2014) 3886.
[25] C.M. Rojas, M. Senthil-Kumar, V. Tzin, K.S. Mysore, Regulation of primary plant metabolism during plant–pathogen interactions and its contribution to plant defense, Front. Plant Sci. 5 (2014) 17.
[26] W. Weckwerth, Integration of metabolomics and proteomics in molecular plant physiology—coping with the complexity by data-dimensionality reduction, Physiol. Plant. 132 (2008) 176–189.
[27] S. Wienkoop, K. Morgenthal, F. Wolschin, M. Scholz, J. Selbig, W. Weckwerth, Integration of metabolomic and proteomic phenotypes: analysis of data covariance dissects starch and RFO metabolism from low and high temperature compensation response in *Arabidopsis thaliana*, Mol. Cell. Proteomics 7 (2008) 1725–1736.
[28] U.K. Aryal, H.L. Xu, M. Fujita, Rhizobia and AM fungal inoculation improve growth and nutrient uptake of bean plants under organic fertilization, J. Sustain. Agric. 21 (2003) 27–39.
[29] D. Harris, R.S. Pacovsky, E.A. Paul, Carbon economy of soybean–*Rhizobium*–*Glomus* associations, New Phytol. 101 (1985) 427–440.
[30] Y. Jia, V.M. Gray, C.J. Straker, The influence of *Rhizobium* and arbuscular mycorrhizal fungi on nitrogen and phosphorus accumulation by *Vicia faba*, Ann. Bot. 94 (2004) 251–258.
[31] Y. Kawai, Y. Yamamoto, Increase in the formation and nitrogen-fixation of soybean nodules by vesicular–arbuscular mycorrhiza, Plant Cell Physiol. 27 (1986) 399–405.
[32] P.E. Mortimer, M.A. Pérez-Fernández, A.J. Valentine, The role of arbuscular mycorrhizal colonization in the carbon and nutrient economy of the tripartite symbiosis with nodulated *Phaseolus vulgaris*, Soil Biol. Biochem. 40 (2008) 1019–1027.
[33] E.A. Paul, R.M. Kucey, Carbon flow in plant microbial associations, Science 213 (1981) 473–474.
[34] D. Bilgin, S. Chandel, Biotic stress globally downregulates photosynthesis genes, Agron. Sustain. Dev. 30 (2010) 581–599.
[35] D. Redecker, P. von Berswordt-Wallrabe, D.P. Beck, D. Werner, Influence of inoculation with arbuscular mycorrhizal fungi on stable isotopes of nitrogen in *Phaseolus vulgaris*, Biol. Fertil. Soils 24 (1997) 344–346.
[36] P.M. Antunes, D. Deaville, M.J. Goss, Effect of two AMF life strategies on the tripartite symbiosis with *Bradyrhizobium japonicum* and soybean, Mycorrhiza 16 (2006) 167–173.
[37] V.I. Franzini, R. Azcon, F.L. Mendes, R. Aroca, Interactions between *Glomus species* and *Rhizobium* strains affect the nutritional physiology of drought-stressed legume hosts, J. Plant Physiol. 167 (2010) 614–619.
[38] T.R. Scheublin, M.G. van der Heijden, Arbuscular mycorrhizal fungi colonize nonfixing root nodules of several legume species, New Phytol. 172 (2006) 732–738.
[39] A. Monzon, R. Azcon, Relevance of mycorrhizal fungal origin and host plant genotype to inducing growth and nutrient uptake in *Medicago* species, Agric. Ecosyst. Environ. 60 (1996) 9–15.
[40] C.A. Atkins, The legume–*Rhizobium* symbiosis—limitations to maximizing nitrogen-fixation, Outlook Agric. 15 (1986) 128–134.
[41] D. Hoffmann, H. Vierheilig, P. Riegler, P. Schausberger, Arbuscular mycorrhizal symbiosis increases host plant acceptance and population growth rates of the two-spotted spider mite *Tetranychus urticae*, Oecologia 158 (2009) 663–671.
[42] W.J. Broughton, M.J. Dilworth, Plant nutrient solutions, in: P. Somasegaran, H.J. Hoben (Eds.), Handbook for Rhizobia; Methods in Legume–*Rhizobium* Technology, Niftal ProjectUniversity of Hawaii, Hawaii 1970, pp. 245–249.
[43] E. Carrillo, D. Rubiales, A. Perez-de-Luque, S. Fondevilla, Characterization of mechanisms of resistance against *Didymella pinodes* in *Pisum* spp. Eur. J. Plant Pathol. 135 (2013) 761–769.
[44] E. Madrid, E. Barilli, J. Gil, T. Huguet, L. Gentzbittel, D. Rubiales, Detection of partial resistance quantitative trait loci against *Didymella pinodes* in *Medicago truncatula*, Mol. Breed. 33 (2013) 589–599.
[45] B. Roger CaT, Effect of culture medium, light and temperature on sexual and asexual reproduction of four strains of *Mycosphaerella pinodes*, Mycol. Res. 100 (1996) 304–306.
[46] H. Vierheilig, A.P. Coughlan, U. Wyss, Y. Piche, Ink and vinegar, a simple staining technique for arbuscular–mycorrhizal fungi, Appl. Environ. Microbiol. 64 (1998) 5004–5007.
[47] E.I. Newman, Citation classic—a method of estimating the total length of root in a sample, Cc/Agric. Biol. Environ. (1981) 18.
[48] M.A. Castillejo, M. Curto, S. Fondevilla, D. Rubiales, J.V. Jorrin, Two-dimensional electrophoresis based proteomic analysis of the pea (*Pisum sativum*) in response to *Mycosphaerella pinodes*, J. Agric. Food Chem. 58 (2010) 12822–12832.
[49] C. Staudinger, V. Mehmeti, R. Turetschek, D. Lyon, V. Egelhofer, S. Wienkoop, Possible role of nutritional priming for early salt and drought stress responses in *Medicago truncatula*, Front. Plant Sci. 3 (2012) 285.

[50] S. Luthje, P. Van Gestelen, M.C. Cordoba-Pedregosa, J.A. Gonzalez-Reyes, H. Asard, J.M. Villalba, et al., Quinones in plant plasma membranes — a missing link? Protoplasma 205 (1998) 43–51.

[51] R. T., A proteomic workflow using high throughput de novo sequencing towards complementation of genome information for improved comparative crop science, in: J. Reinders (Ed.) Proteomics in Symstemy BiologySpringer, 2015.

[52] J. Cox, M. Mann, MaxQuant enables high peptide identification rates, individualized p.p.b.-range mass accuracies and proteome-wide protein quantification, Nat. Biotechnol. 26 (2008) 1367–1372.

[53] Team RDC, R: A Language and Environment for Statistical Computing. Vienna, Austria: The R Foundation for Statistical Computing, 2011, ISBN 3-900051-07-0 (Available online at http://www.r-project.org/).

[54] G.R. Warnes, B. Bolker, L. Bonebakker, R. Gentleman, W. Huber, A. Liaw, et al., gplots: Various R Programming Tools for Plotting Data. R Package Version, 2009 2.

[55] E. N. Neuwirth. RColorBrewer: ColorBrewer Palettes. R Package Version 1.0-22007.

[56] M. Lohse, A. Nagel, T. Herter, P. May, M. Schroda, R. Zrenner, et al., Mercator: a fast and simple web server for genome scale functional annotation of plant sequence data, Plant Cell Environ. 37 (2014) 1250–1258.

[57] Z. Du, X. Zhou, Y. Ling, Z.H. Zhang, Z. Su, agriGO: a GO analysis toolkit for the agricultural community, Nucleic Acids Res. 38 (2010) W64–W70.

[58] E. Alexandersson, G. Saalbach, C. Larsson, P. Kjellbom, *Arabidopsis* plasma membrane proteomics identifies components of transport, signal transduction and membrane trafficking, Plant Cell Physiol. 45 (2004) 1543–1556.

[59] R. Zhang, S.F. Hwang, K.F. Chang, S.E. Strelkov, R.J. Howard, Comparative proteomics of systemic resistance in genotypes of *Pisum sativum* attacked by *Mycosphaerella pinodes*, Can. J. Plant Pathol. 28 (2006) 321–322.

[60] D.J. Angelopoulou, E.J. Naska, E.J. Paplomatas, S.E. Tjamos, Biological control agents (BCAs) of verticillium wilt: influence of application rates and delivery method on plant protection, triggering of host defence mechanisms and rhizosphere populations of BCAs, Plant Pathol. 63 (2014) 1062–1069.

[61] S. Rospert, Y. Dubaquie, M. Gautschi, Nascent-polypeptide-associated complex, Cell. Mol. Life Sci. 59 (2002) 1632–1639.

[62] S. Schaarschmidt, P.M. Gresshoff, B. Hause, Analyzing the soybean transcriptome during autoregulation of mycorrhization identifies the transcription factors GmNF-YA1a/b as positive regulators of arbuscular mycorrhization, Genome Biol. 14 (2013) R62.

[63] N. Allsopp, W.D. Stock, Density dependent interactions between VA mycorrhizal fungi and even-aged seedlings of two perennial Fabaceae species, Oecologia 91 (1992) 281–287.

[64] R.T. Koide, Density-dependent response to mycorrhizal infection in *Abutilon-theophrasti* Medic, Oecologia 85 (1991) 389–395.

[65] X. Gao, X. Lu, M. Wu, H.Y. Zhang, R.Q. Pan, J. Tian, et al., Co-inoculation with rhizobia and AMF inhibited soybean red crown rot: from field study to plant defense-related gene expression analysis, PLoS One 7 (2012).

[66] M. Geneva, G. Zehirov, E. Djonova, N. Kaloyanova, G. Georgiev, I. Stancheva, The effect of inoculation of pea plants with mycorrhizal fungi and *Rhizobium* on nitrogen and phosphorus assimilation, Plant Soil Environ. 52 (2006) 435–440.

[67] S. Reinhard, P. Martin, H. Marschner, Interactions in the tripartite symbiosis of pea (*Pisum-sativum* L), *Glomus* and *Rhizobium* under nonlimiting phosphorus supply, J. Plant Physiol. 141 (1993) 7–11.

[68] A.L. Larimer, K. Clay, J.D. Bever, Synergism and context dependency of interactions between arbuscular mycorrhizal fungi and rhizobia with a prairie legume, Ecology 95 (2014) 1045–1054.

[69] F. Tajini, M. Trabelsi, J.J. Drevon, Combined inoculation with *Glomus intraradices* and *Rhizobium tropici* CIAT899 increases phosphorus use efficiency for symbiotic nitrogen fixation in common bean (*Phaseolus vulgaris* L.), Saudi J. Biol. Sci. 19 (2012) 157–163.

[70] B. Hause, W. Maier, O. Miersch, R. Kramell, D. Strack, Induction of jasmonate biosynthesis in arbuscular mycorrhizal barley roots, Plant Physiol. 130 (2002) 1213–1220.

[71] A. Nair, S.P. Kolet, H.V. Thulasiram, S. Bhargava, Systemic jasmonic acid modulation in mycorrhizal tomato plants and its role in induced resistance against *Alternaria alternata*, Plant Biol. (Stuttg.) 17 (2015) 625–631.

[72] H.S. Seo, J. Li, S.Y. Lee, J.W. Yu, K.H. Kim, S.H. Lee, et al., The hypernodulating nts mutation induces jasmonate synthetic pathway in soybean leaves, Mol. Cells 24 (2007) 185–193.

[73] M. Kinkema, P.M. Gresshoff, Investigation of downstream signals of the soybean autoregulation of nodulation receptor kinase GmNARK, Mol. Plant-Microbe Interact. 21 (2008) 1337–1348.

[74] S. Isayenkov, C. Mrosk, I. Stenzel, D. Strack, B. Hause, Suppression of allene oxide cyclase in hairy roots of *Medicago truncatula* reduces jasmonate levels and the degree of mycorrhization with *Glomus intraradices*, Plant Physiol. 139 (2005) 1401–1410.

[75] E.T. Kiers, L.S. Adler, E.L. Grman, M.G.A. van der Heijden, Manipulating the jasmonate response: how do methyl jasmonate additions mediate characteristics of aboveground and belowground mutualisms? Funct. Ecol. 24 (2010) 434–443.

[76] J.M. Plett, A. Khachane, M. Ouassou, B. Sundberg, A. Kohler, F. Martin, Ethylene and jasmonic acid act as negative modulators during mutualistic symbiosis between *Laccaria bicolor* and *Populus* roots, New Phytol. 202 (2014) 270–286.

[77] Shiraishi Tomonori, Oku Hachiro, Tsuji Yoshio, O. S., Inhibitory effect of pisatin on infection process of *Mycosphaerella pinodes* on pea, Ann. Phytopathol. Soc. Jpn. 44 (1978) 641–645.

[78] M.A. Ponce, J.M. Scervino, R. Erra-Balsells, J.A. Ocampo, A.M. Godeas, Flavonoids from shoots and roots of *Trifolium repens* (white clover) grown in presence or absence of the arbuscular mycorrhizal fungus *Glomus intraradices*, Phytochemistry 65 (2004) 1925–1930.

[79] A. Aloui, G. Recorbet, F. Robert, B. Schoefs, M. Bertrand, C. Henry, et al., Arbuscular mycorrhizal symbiosis elicits shoot proteome changes that are modified during cadmium stress alleviation in *Medicago truncatula*, BMC Plant Biol. 11 (2011) 75.

[80] C. Poschenrieder, R. Tolra, J. Barcelo, Can metals defend plants against biotic stress? Trends Plant Sci. 11 (2006) 288–295.

[81] K.M. Jones, H. Kobayashi, B.W. Davies, M.E. Taga, G.C. Walker, How rhizobial symbionts invade plants: the *Sinorhizobium–Medicago* model, Nat. Rev. Microbiol. 5 (2007) 619–633.

[82] M.R. Pereira, B.C. Gouvêa, F.C. Marcelino-Guimarães, HJdO Ramos, M.A. Moreira, EGd Barros, Proteomic analysis of soybean leaves in a compatible and an incompatible interaction with phakopsora pachyrhizi, Organelles Proteomics 1 (2014).

[83] Y.T. Zhang, Y.L. Zhang, S.X. Chen, G.H. Yin, Z.Z. Yang, S. Lee, et al., Proteomics of methyl jasmonate induced defense response in maize leaves against Asian corn borer, BMC Genomics 16 (2015).

[84] X.Q. Zheng, C. Nagai, H. Ashihara, Pyridine nucleotide cycle and trigonelline (*N*-methylnicotinic acid) synthesis in developing leaves and fruits of *Coffea arabica*, Physiol. Plant. 122 (2004) 404–411.

[85] S.N. Hashida, T. Itami, H. Takahashi, K. Takahara, M. Nagano, M. Kawai-Yamada, et al., Nicotinate/nicotinamide mononucleotide adenyltransferase-mediated regulation of NAD biosynthesis protects guard cells from reactive oxygen species in ABA-mediated stomatal movement in *Arabidopsis*, J. Exp. Bot. 61 (2010) 3813–3825.

[86] C. Dutilleul, M. Garmier, G. Noctor, C. Mathieu, P. Chetrit, C.H. Foyer, et al., Leaf mitochondria modulate whole cell redox homeostasis, set antioxidant capacity, and determine stress resistance through altered signaling and diurnal regulation, Plant Cell 15 (2003) 1212–1226.

[87] A.A.A. Latef, Influence of arbuscular mycorrhizal fungi and copper on growth, accumulation of osmolyte, mineral nutrition and antioxidant enzyme activity of pepper (*Capsicum annuum* L.), Mycorrhiza 21 (2011) 495–503.

[88] M. Miransari, Hyperaccumulators, arbuscular mycorrhizal fungi and stress of heavy metals, Biotechnol. Adv. 29 (2011) 645–653.

[89] A. Schutzendubel, A. Polle, Plant responses to abiotic stresses: heavy metal-induced oxidative stress and protection by mycorrhization, J. Exp. Bot. 53 (2002) 1351–1365.

[90] U.W. Stephan, G. Scholz, Nicotianamine — mediator of transport of iron and heavy-metals in the phloem? Physiol. Plant. 88 (1993) 522–529.

[91] N. von Wiren, S. Klair, S. Bansal, J.F. Briat, H. Khodr, T. Shioiri, et al., Nicotianamine chelates both Fe-III and Fe-II. Implications for metal transport in plants, Plant Physiol. 119 (1999) 1107–1114.

[92] K. Ravet, B. Touraine, J. Boucherez, J.F. Briat, F. Gaymard, F. Cellier, Ferritins control interaction between iron homeostasis and oxidative stress in *Arabidopsis*, Plant J. 57 (2009) 400–412.

[93] D. Wipf, G. Mongelard, D. van Tuinen, L. Gutierrez, L. Casieri, Transcriptional responses of *Medicago truncatula* upon sulfur deficiency stress and arbuscular mycorrhizal symbiosis, Front. Plant Sci. 5 (2014).

[94] A. Lebrun-Garcia, S. Bourque, M.N. Binet, F. Ouaked, D. Wendehenne, A. Chiltz, et al., Involvement of plasma membrane proteins in plant defense responses. Analysis of the cryptogein signal transduction in tobacco, Biochimie 81 (1999) 663–668.

[95] C.C. Chiang, L.A. Hadwiger, Cloning and characterization of a disease resistance response gene in pea inducible by *Fusarium solani*, Mol. Plant-Microbe Interact. 3 (1990) 78–85.

[96] D.E. Culley, D. Horovitz, L.A. Hadwiger, Molecular characterization of disease-resistance response gene DRR206-d from *Pisum sativum* (L.), Plant Physiol. 107 (1995) 301–302.

[97] M.A. Castillejo, M. Fernandez-Aparicio, D. Rubiales, Proteomic analysis by two-dimensional differential in gel electrophoresis (2D DIGE) of the early response of *Pisum sativum* to *Orobanche crenata*, J. Exp. Bot. 63 (2012) 107–119.

[98] S. Hosseini, M. Elfstrand, F. Heyman, D. Funck Jensen, M. Karlsson, Deciphering common and specific transcriptional immune responses in pea towards the oomycete pathogens *Aphanomyces euteiches* and *Phytophthora pisi*, BMC Genomics 16 (2015) 627.

[99] J.M. Ruiz-Lozano, H. Roussel, S. Gianinazzi, V. Gianinazzi-Pearson, Defense genes are differentially induced by a mycorrhizal fungus and *Rhizobium* sp. in wild-type and symbiosis-defective pea genotypes, Mol. Plant-Microbe Interact. 12 (1999) 976–984.

[100] T. Kinoshita, M. Nishimura, K.I. Shimazaki, Cytosolic concentration of Ca^{2+} regulates the plasma-membrane H^{+}-ATPase in guard-cells of fava bean, Plant Cell 7 (1995) 1333–1342.

[101] H. Batoko, A. de Kerchove d'Exaerde, J.M. Kinet, J. Bouharmont, R.A. Gage, H. Maraite, et al., Modulation of plant plasma membrane H^{+}-ATPase by phytotoxic lipodepsipeptides produced by the plant pathogen *Pseudomonas fuscovaginae*, Biochim. Biophys. Acta 1372 (1998) 216–226.

[102] J. Kurepa, S. Wang, Y. Li, J. Smalle, Proteasome regulation, plant growth and stress tolerance, Plant Signal. Behav. 4 (2009) 924–927.

[103] G. Fabro, I. Kovacs, V. Pavet, L. Szabados, M.E. Alvarez, Proline accumulation and AtP5CS2 gene activation are induced by plant–pathogen incompatible interactions in *Arabidopsis*, Mol. Plant-Microbe Interact. 17 (2004) 343–350.

[104] S. Hayat, Q. Hayat, M.N. Alyemeni, A.S. Wani, J. Pichtel, A. Ahmad, Role of proline under changing environments: a review, Plant Signal. Behav. 7 (2012) 1456–1466.

[105] M.A. Castillejo, M. Bani, D. Rubiales, Understanding pea resistance mechanisms in response to *Fusarium oxysporum* through proteomic analysis, Phytochemistry 115 (2015) 44–58.

[106] A. Mhamdi, C. Mauve, H. Gouia, P. Saindrenan, M. Hodges, G. Noctor, Cytosolic NADP-dependent isocitrate dehydrogenase contributes to redox homeostasis

and the regulation of pathogen responses in *Arabidopsis* leaves, Plant Cell Environ. 33 (2010) 1112–1123.
[107] M.J. Hynes, S.L. Murray, ATP-citrate lyase is required for production of cytosolic acetyl coenzyme A and development in *Aspergillus nidulans*, Eukaryot. Cell 9 (2010) 1039–1048.
[108] D. Rangasamy, C. Ratledge, Compartmentation of ATP:citrate lyase in plants, Plant Physiol. 122 (2000) 1225–1230.
[109] S. Prisic, M. Xu, P.R. Wilderman, R.J. Peters, Rice contains two disparate *ent*-copalyl diphosphate synthases with distinct metabolic functions, Plant Physiol. 136 (2004) 4228–4236.
[110] A.R. Jassbi, K. Gase, C. Hettenhausen, A. Schmidt, I.T. Baldwin, Silencing geranylgeranyl diphosphate synthase in *Nicotiana attenuata* dramatically impairs resistance to tobacco hornworm, Plant Physiol. 146 (2008) 974–986.
[111] H. Jornvall, B. Persson, M. Krook, S. Atrian, R. Gonzalez-Duarte, J. Jeffery, et al., Short-chain dehydrogenases/reductases (SDR), Biochemistry 34 (1995) 6003–6013.
[112] S.G. Hwang, N.C. Lin, Y.Y. Hsiao, C.H. Kuo, P.F. Chang, W.L. Deng, et al., The *Arabidopsis* short-chain dehydrogenase/reductase 3, an abscisic acid deficient 2 homolog, is involved in plant defense responses but not in ABA biosynthesis, Plant Physiol. Biochem. 51 (2012) 63–73.
[113] C.J. Howe, M.M. Lahair, J.A. McCubrey, R.A. Franklin, Redox regulation of the calcium/calmodulin-dependent protein kinases, J. Biol. Chem. 279 (2004) 44573–44581.
[114] J. Chen, C. Gutjahr, A. Bleckmann, T. Dresselhaus, Calcium signaling during reproduction and biotrophic fungal interactions in plants, Mol. Plant 8 (2015) 595–611.
[115] H. Feng, X. Wang, Y. Sun, X. Wang, X. Chen, J. Guo, et al., Cloning and characterization of a calcium binding EF-hand protein gene TaCab1 from wheat and its expression in response to *Puccinia striiformis* f. sp. *tritici* and abiotic stresses, Mol. Biol. Rep. 38 (2011) 3857–3866.
[116] M.C. Kim, R. Panstruga, C. Elliott, J. Muller, A. Devoto, H.W. Yoon, et al., Calmodulin interacts with MLO protein to regulate defence against mildew in barley, Nature 416 (2002) 447–451.
[117] V.A. Halim, A. Vess, D. Scheel, S. Rosahl, The role of salicylic acid and jasmonic acid in pathogen defence, Plant Biol. (Stuttg.) 8 (2006) 307–313.
[118] C.M. Pieterse, D. Van der Does, C. Zamioudis, A. Leon-Reyes, S.C. Van Wees, Hormonal modulation of plant immunity, Annu. Rev. Cell Dev. Biol. 28 (2012) 489–521.
[119] C. Zamioudis, C.M. Pieterse, Modulation of host immunity by beneficial microbes, Mol. Plant-Microbe Interact. 25 (2012) 139–150.
[120] M. Rapala-Kozik, N. Wolak, M. Kujda, A.K. Banas, The upregulation of thiamine (vitamin B1) biosynthesis in *Arabidopsis thaliana* seedlings under salt and osmotic stress conditions is mediated by abscisic acid at the early stages of this stress response, BMC Plant Biol. 12 (2012) 2.
[121] E.A. Iturriaga, M.J. Leech, D.H. Barratt, T.L. Wang, Two ABA-responsive proteins from pea (*Pisum sativum* L.) are closely related to intracellular pathogenesis-related proteins, Plant Mol. Biol. 24 (1994) 235–240.
[122] S.A. Clulow, B.G. Lewis, P. Matthews, Expression of resistance to *Mycosphaerella pinodes* in *Pisum sativum*, Plant Pathol. 41 (1992) 362–369.
[123] J.M. Wroth, Possible role for wild genotypes of *Pisum* spp. to enhance ascochyta blight resistance in pea, Aust. J. Exp. Agric. 38 (1998).
[124] A.P. Maloney, H.D. Vanetten, A gene from the fungal plant pathogen nectria-haematococca that encodes the phytoalexin-detoxifying enzyme pisatin demethylase defines a new cytochrome-P450 family, Mol. Gen. Genet. 243 (1994) 506–514.
[125] S.C. Van Wees, S. Van der Ent, C.M. Pieterse, Plant immune responses triggered by beneficial microbes, Curr. Opin. Plant Biol. 11 (2008) 443–448.
[126] A.P.G. Prime, U. Conrath, G.J. Beckers, V. Flors, P. Garcia-Agustin, G. Jakab, et al., Priming: getting ready for battle, Mol. Plant-Microbe Interact. 19 (2006) 1062–1071.
[127] V. Doubnerova Hyskova, L. Miedzinska, J. Dobra, R. Vankova, H. Ryslava, Phosphoenolpyruvate carboxylase, NADP-malic enzyme, and pyruvate, phosphate dikinase are involved in the acclimation of *Nicotiana tabacum* L. to drought stress, J. Plant Physiol. 171 (2014) 19–25.
[128] B.J. Shelp, A.W. Bown, M.D. McLean, Metabolism and functions of gamma-aminobutyric acid, Trends Plant Sci. 4 (1999) 446–452.
[129] S. Sulieman, Does GABA increase the efficiency of symbiotic N_2 fixation in legumes? Plant Signal. Behav. 6 (2011) 32–36.
[130] S. Sulieman, J. Schulze, Phloem-derived gamma-aminobutyric acid (GABA) is involved in upregulating nodule N_2 fixation efficiency in the model legume *Medicago truncatula*, Plant Cell Environ. 33 (2010) 2162–2172.
[131] Y. Takenaka, S. Nakano, M. Tamoi, S. Sakuda, T. Fukamizo, Chitinase gene expression in response to environmental stresses in *Arabidopsis thaliana*: chitinase inhibitor allosamidin enhances stress tolerance, Biosci. Biotechnol. Biochem. 73 (2009) 1066–1071.
[132] E. Aglika, Pathogenesis-related proteins: research progress in the last 15 years, Gen. Appl. Plant Physiol. 31 (2005) 105–124.
[133] S. Pereira Menezes, E.M. de Andrade Silva, E. Matos Lima, A. Oliveira de Sousa, B. Silva Andrade, L. Santos Lima Lemos, et al., The pathogenesis-related protein PR-4b from *Theobroma cacao* presents RNase activity, Ca^{2+} and Mg^{2+} dependent-DNase activity and antifungal action on *Moniliophthora perniciosa*, BMC Plant Biol. 14 (2014) 161.
[134] I.A. Penninckx, K. Eggermont, F.R. Terras, B.P. Thomma, G.W. De Samblanx, A. Buchala, et al., Pathogen-induced systemic activation of a plant defensin gene in *Arabidopsis* follows a salicylic acid-independent pathway, Plant Cell 8 (1996) 2309–2323.
[135] X. Wang, C. Tang, L. Deng, G. Cai, X. Liu, B. Liu, et al., Characterization of a pathogenesis-related thaumatin-like protein gene TaPR5 from wheat induced by stripe rust fungus, Physiol. Plant. 139 (2010) 27–38.